Department of Structural Engineering
Danmarks Tekniske Højskole · Technical University of Denmark

Creep and Shrinkage of High-Strength Concrete; An analysis

Henrik Elgaard Jensen

Serie R No 294 1992

Creep and Shrinkage of High-Strength Concrete; An Analysis

Tryk:
Afdelingen for Bærende Konstruktioner
Danmarks Tekniske Højskole
Lyngby
ISBN 87-7740-115-8

Preface

This report is a part of the research project "High Performance Concretes in the 90's". The report is an analysis of the test results presented in the report "Creep and Shrinkage of High-Strength Concrete; A test report".

The research project has been carried out at the Department of Structural Engineering, Technical University of Denmark. The project has been carried out under the supervision of Professor Mogens Peter Nielsen.

The project consist of 3 reports of which the present report is the final report.

1. State-of-the-art rapport for Højstyrkebetons svind og krybning.

2. Creep and Shrinkage of High-Strength Concrete; A Test Report. + Appendices A-D.

3. Creep and Shrinkage of High-Strength Concrete; An Analysis.

The entire project has been financed by the "Industri- og Handelsstyrelsen".

Henrik Stang and Torben Valdbjørn Rasmussen applied the thin-section analyses, for which I am very grateful.

I thank Matthew Bloomstine and Karin Kaderková who have revised the manuscript.

A lot of people and departments, mentioned and not mentioned, have contributed assistance or advise to the project. I would like to express my deep gratitude to everyone who helped make this project become a reality.

May 1992

Henrik Elgaard Jensen

I. Abstract

The research project has been carried out as a Ph.D. study at the Department of Structural Engineering, Technical University of Denmark. The supervisor of the Ph.D. study has been Professor Dr. techn. Mogens Peter Nielsen.

The Ph.D. Thesis consist of 3 theses performed during the period of the Ph.D. study:

1. State-of-the-art rapport for Højstyrkebetons svind og krybning.

2. Creep and Shrinkage of High-Strength Concrete; A Test Report. + Appendices A-D.

3. Creep and Shrinkage of High-Strength Concrete; An Analysis.

1. State-of-the-art rapport for Højstyrkebetons svind og krybning.

The report deals briefly with the concepts and models which are used in relation to shrinkage and creep of concrete.
Different kinds of test-equipment are evaluated for usage in the experimental part of the project.
A review of the ingredients which are used to produce a high-strength concrete and the influence of these ingredients on shrinkage and creep of concrete, are obtained by references to tests reported in the literature.

2. Creep and Shrinkage of High-Strength Concrete; A Test Report. + Appendices A-D.

The investigation deals with some time-dependent mechanical properties of seven different concretes. The time-dependent properties are shrinkage, uniaxial-creep and aging. The compressive strength of the seven concretes vary from 10 Mpa to 100 Mpa.
The concretes are exposed to drying at a temperature of 21 °C and a relative humidity of 65 % after 28 days of water curing. The stress/strength ratio is 1/3 in the creep tests.
Three of the seven concretes are investigated further. The compressive strength of the three

concretes is 15, 80 and 100 MPa.
The stress/strength ratio is varied from 0.4 to 0.7 for the three concretes in different creep tests. The three concretes are also investigated under sealed conditions, and after a water curing period of 7 days.
The pastes of the 80 and 100 MPa concretes are investigated as well, and creep recovery of the three concretes are studied.
The period of measuring is at least 11 month for all tests.

3. Creep and Shrinkage of High-Strength Concrete; An Analysis.

This is a qualitative analysis of the test results presented in the test report. The analysis concerns a qualitative evaluation of the general mechanical properties and the time-dependent mechanical properties shrinkage, creep, weight-loss, development of strength/stiffness, age at loading, stress/strength ratio, microcracking, drying creep, static-fatigue and creep recovery. Based upon the analysis it is demonstrated that high-strength/high-performance concrete, containing microsilica fume and/or fly-ash and plasticizer, is not a new material with respect to the investigated properties.
The investigated concretes exhibit mechanical properties which comply with existing knowledge of the mechanisms of creep and shrinkage.
To avoid misinterpretations related to test conditions, the test results are evaluated quantitatively in relation to the "CEB-FIP modelcode 1990". The modelcode is used as a mathematical standard of test evaluation, as the CEB-FIP modelcode 1990 is calibrated by means of a computerized data bank to fit several shrinkage and creep laboratory tests.

Keywords: Drying creep, basic creep, shrinkage, aging, testing, high-strength concrete, high stress/strength-level, creep recovery.

1. Resumé

Forskningsprojektet er gennemført som et licentiat studium på Afdelingen for Bærende Konstruktioner, Danmarks tekniske Højskole. Licentiat studiets vejleder har været Professor Dr. Techn. Mogens Peter Nielsen.

Licentiat afhandlingen består af 3 afhandlinger udført gennem licentiat studiet:

1. State-of-the-art rapport for Højstyrkebetons svind og krybning.
2. Creep and Shrinkage of High-Strength Concrete; A Test Report. + Appendices A-D.
3. Creep and Shrinkage of High-Strength Concrete; An Analysis.

1. State-of-the-art rapport for Højstyrkebetons svind og krybning.

Rapporten omhandler kort de begreber og modeller, der benyttes i forbindelse med betons svind og krybning.
Forskellige typer forsøgsudstyr er vurderet med henblik på senere brug i den eksperimentelle del af det samlede projekt.
Der gives et overblik over de ingredienser, der benyttes ved produktion af højstyrkebeton og disse ingrediensers indflydelse på betons svind- og krybeegenskaber, ved reference til forsøg indsamlet fra litteraturen om emnet.

2. Creep and Shrinkage of High-Strength Concrete; A Test Report. + Appendices A-D.

Undersøgelsen omhandler nogle tidsafhængige mekaniske egenskaber for syv forskellige betoner.
De tidsafhængige egenskaber er svind, eenakset-krybning og ældning. Trykstyrken af de syv betoner varierer fra 10 MPa til 100 MPa.
Betonerne er udsat for udtørring ved 21 °C og ved en relativ luftfugtighed på 65 % efter 28 dg. vandlagring. Spændings/styrke forholdet er 1/3 i krybeforsøgene.

Tre af betonerne er undersøgt yderligere. Trykstyrken af de tre betoner er 15, 80 og 100 MPa. Spændings/styrke forholdet er varieret fra 0.4 til 0.7 for de tre betoner i forskellige krybeforsøg. De tre betoner er også undersøgt under forseglede forhold og efter en vandlagringsperiode på 7 dage.
80 og 100 MPa betonernes pasta er ligeledes undersøgt og tilbagekrybningen er undersøgt for de tre betoner.
Måleperioden er mindst 11 måneder for alle forsøg.

3. Creep and Shrinkage of High-Strength Concrete; An Analysis.

Dette er en kvalitativ analyse af de forsøgsresultater, der er præsenteret i forsøgsrapporten. Analysen er en kvalitativ vurdering af de generelle mekaniske egenskaber og de tidsafhængige mekaniske egenskaber som svind, krybning, vægttab, udvikling af styrke/stivhed, belastningsalder, spændings/styrke forhold, mikrorevner, udtørrings krybning, langtidsstyrke og tilbagekrybning. På baggrund af analysen er det vist, at højstyrke-/højkvalitetsbeton, der indeholder mikrosilica og/eller flyveaske og plastificerende midler, ikke er et nyt materiale med hensyn til de undersøgte egenskaber.
De undersøgte betoner udviser mekaniske egenskaber, der stemmer overens med eksisterende viden om svind- og krybemekanismerne.
For at undgå fejlfortolkninger relateret til forsøgsbetingelser, er forsøgsresultaterne vurderet kvantitativt i forhold til "CEB-FIP modelcode 1990". Modelnormen er brugt som en matematisk standard til forsøgsvurdering, da CEB-FIP modelcode er kalibreret vha. en EDB data bank mht. svind og krybning bestemt ved laboratorieforsøg.

Nøgleord: Udtørringskrybning, grundkrybning, svind, ældning, forsøg, højstyrke beton, højt spændings/styrke niveau, tilbagekrybning.

II. LIST OF CONTENTS

III. LIST OF SYMBOLS

ϵ	Strain
ϵ_σ	Strain at the corresponding creep stress-level
ϵ_0	Initial strain
ϵ_{cr}	Creep strain
ϵ_{sh}	Shrinkage strain
ϵ_{total}	Total strain
$\mu\epsilon$	Micro strain
ρ	Density
σ	Stress
φ	Creep coefficient
υ	Poisson ratio
c	Specific creep
d	Specific deformation
E	Elastic-modulus
$E_{\sigma 0}$	Initial elastic-modulus at a certain stress
E_0	Initial elastic-modulus
E_{dyn}	Dynamic modulus
E_s	Initial secant-modulus
f_c	Compressive strength
f_{c0}	Compressive strength at the time of creep-loading
g	Aggregate content
l	Length
t	Time
t_0	Age at loading

SHORTENINGS

HSC	High-Strength-Concrete	60-85 MPa
LSC	Low-Strength-Concrete	10-30 MPa
NSC	Normal-Strength-Concrete	30-60 MPa
VLSC	Very-Low-Strength-Concrete	0-10 MPa
VHSC	Very-High-Strength-Concrete	85-110 MPa

1 INTRODUCTION

This introduction concerns the factors which affect shrinkage and creep and the mechanisms of shrinkage and creep. The scope of the introduction is to emphasize the difficulty of determining the influence of just one parameter affecting creep and shrinkage.
Many questions concerning the mechanisms of shrinkage and creep still remain unanswered and the introduction is just a brief review of the status quo.
A hypothesis concerning drying creep as a consequence of microcracking is presented in the introduction.
The following sections are an analysis of the test results reported in [92.1].

1.1 Factors affecting Shrinkage

An unloaded and unrestrained concrete specimen undergoes a volume change with time. The volume change is caused by the exchange of water between the concrete and the environment surrounding the concrete or by formation of new cement gel using evaporable- or gelwater inside the concrete. The volume change is 3 times the linear deformation [86.6] and recognized as shrinkage. The linear shrinkage is the parameter which is usually determined in shrinkage tests.
A concrete specimen which is in hydrostatic equilibrium with the ambience does not exhibit shrinkage.The time before natural hydrostatic equilibrium is reached can be relatively long, i.e. 1 to 2 years for a Ø100 x 200 mm cylinder exposed to drying at a relative humidity of 65 % after 28 days of water curing.
Most factors which affect shrinkage affect creep too and the consequence of the effect is similar to the effect on creep.
The most significant factors which affect shrinkage are:

1. The water/cement ratio.
2. The mechanical properties of the aggregate and the aggregate/paste ratio.
3. The mechanical properties of the cement paste.
4. The environmental conditions.
5. The presence and development of cracks.
6. The age at the start of water exchange.
7. The development of the mechanical properties.

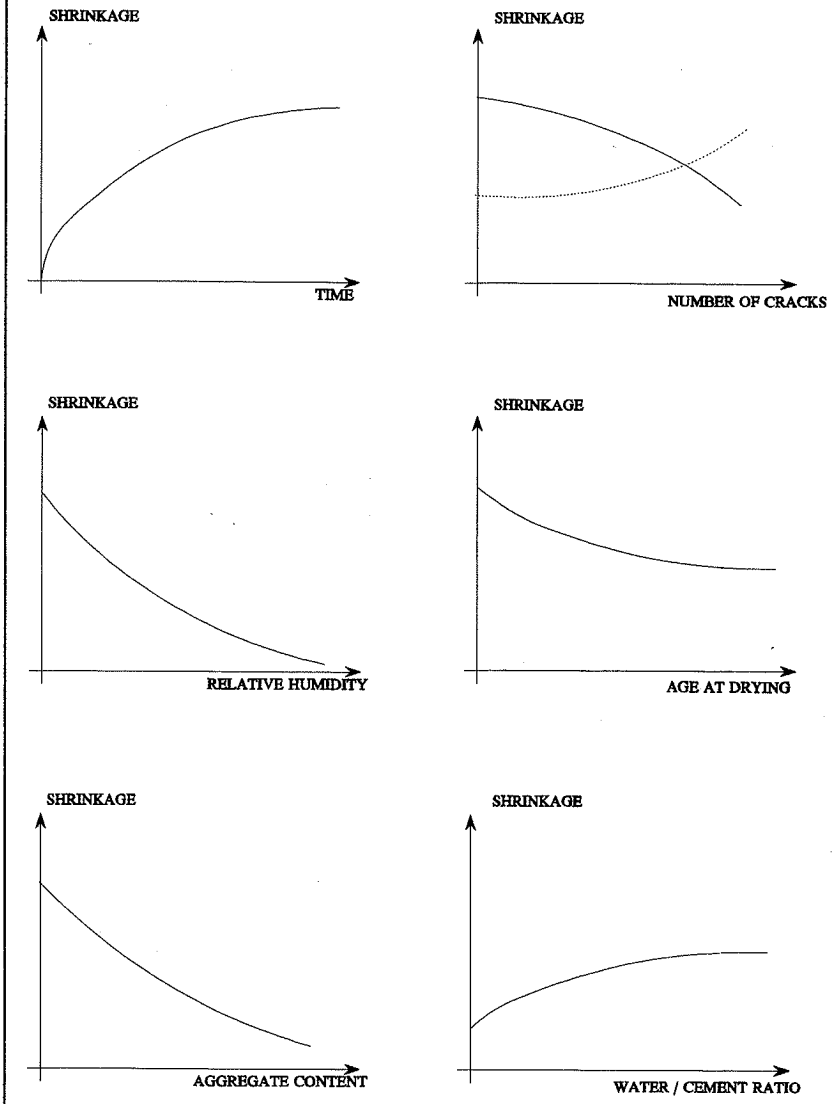

Fig. 1.1 Schematic illustration of the relationship between shrinkage and some of the factors influencing shrinkage.

In Fig. 1.1 the relationship between shrinkage and some of the factors influencing shrinkage is illustrated schematically.
The cement paste is the main cause of concrete shrinkage. Many time-dependent properties can be traced to the cement paste.
As the water/cement ratio is increased the porosity of the cement is increased too. A high porosity improves the ability of internal migration of water. A high water/cement ratio also leaves more water which is not used for hydration of the cement. The more free evaporable water the more shrinkage, and the easier the water can leave the concrete the higher the shrinkage rate.

Shrinkage of concrete is restrained shrinkage. The aggregate of the concrete restrain the shrinkage of the cement paste. The restraint is related to the mechanical properties of the aggregate and the aggregate/paste ratio. The consequence of the restraint by the aggregate is that the aggregate is in a state of compression and the cement paste is in a state of tension. The restraint can cause tensile stresses which exceed the tensile strength of the cement paste, in which case cracks are developed in the cement paste. The tensile stresses in the cement paste are relieved by creep. The presence of cracks improves the ability of the water to migrate inside the concrete.
An increased aggregate/paste ratio decreases the shrinkage in an order of {1.1}.

$$\varepsilon_{sh,concrete} = (1 - g)^n \cdot \varepsilon_{sh,paste} \qquad \{1.1\}$$

$\epsilon_{sh,concrete}$	Shrinkage of concrete
g	Aggregate content
$\epsilon_{sh,paste}$	Shrinkage of neat cement paste
n	1.7 according to Pickett [56.1] but is dependent on the mechanical properties of the aggregate.

The influence of the relative humidity is obviously a dominant factor on shrinkage. As the humidity of the environmental surroundings is decreased the shrinkage is increased.
Usually the relative humidity of the environment is responsible for most of the shrinkage. Concretes with water/cement ratios less than 0.5 do exhibit an increased autogenous shrinkage in relation to ordinary concretes. The increase of the autogenous shrinkage is caused by the cement's use of gelwater for hydration. Concretes with water/cement ratios less than 0.4 is not able to hydrate the entire cement content. The result of this excess of cement is an enhanced consumption of water physically available for hydration. The consequence of this mechanism is a decrease of the relative humidity inside the concrete. This phenomena is called

selfdesiccation and the physical mechanism is identical to drying shrinkage and causes an increased shrinkage. The range of magnitude of the autogenous shrinkage is 50-100 $\mu\epsilon$.

The sooner the concrete is exposed to drying the more shrinkage can usually be observed. The increased shrinkage at early age drying is due to the unfinished hydration, as there is a relatively high amount of evaporable water during the early stages of hydration. The influences of curing and the duration of curing are rather complex and is not yet quite identified.
The influence of the development of mechanical properties (aging) is more significant during the early stages of hydration. The older the concrete the less creep can relieve tensile stresses caused by shrinkage.

1.2 Factors affecting creep

It is a known fact that if a constant load is applied to a concrete specimen that it will continue to deform for a long period of time in addition to the initial deformation. It is believed that the deformation in fact does not stop. This deformation is known as creep.
A lot of building materials exhibit creep during a period of sustained loading e.g. wood, soil, steel, concrete, etc.
A material like steel creeps when the load-level is close to the yield stress. The mechanism of steel creep is due to slipping along planes within the material. When a material like steel creeps usually a failure will arise. Materials like wood, soil and concrete do not necessarily fail during a long period of creep. Creep of wood, soil and concrete is due to the presence of water in the fine pores of the material.
Concrete creep is a far more complex problem than e.g. creep of soil because the basic mechanical properties of concrete change during the creep period due to hydration.
The main factors influencing creep are:

1. The water/cement ratio.
2. The mechanical properties of the aggregate and the aggregate/paste ratio.
3. The mechanical properties of the cement paste.
4. The environmental conditions.
5. The presence and development of cracks.
6. The stress/strength ratio.
7. The age at loading.

In Fig. 1.2 the relationship between creep and some of the factors influencing creep is illustrated schematically.

Most of the factors influence shrinkage as well and the two phenomena are interrelated. Some theories even claim that creep is just a load-induced shrinkage. The 8 factors mentioned are more or less interrelated in their effect on concrete creep.

A decrease of the water/cement ratio increases the strength. The creep decreases when the strength is increased. The porosity of the paste is influenced by the water/cement ratio and the porosity affects the mechanical properties of the cement paste.

As the paste creeps, more and more of the applied load is transferred to the aggregate. The interaction between the cement paste and the aggregate depends upon the mechanical properties of the two materials and the aggregate/paste ratio.

Environmental conditions, such as the relative humidity, influence creep. The influence of the relative humidity is related to the porosity of the concrete. The possibility to evaporate water and of interior transport of water to the surface of the concrete is related to the porosity and illustrates that the size and shape of the specimen influence creep and shrinkage in the same order of magnitude. The external stress is believed to compress the pores of the concrete and thus slow down the transport of water to the concrete surface [90.4].

The development of cracks and the presence of cracks in the concrete has a significant influence on the stress-strain curve and creep. Cracks can be caused by shrinkage or an external load. Shrinkage and creep cause new cracks and increase existing cracks during the creep period. Introducing a new crack or increasing an existing crack requires that the tensile strength has been exceeded. The tensile strength is related to the water/cement ratio.

Creep is caused by a state of stress, the stress can be external or intrinsic. Creep is increased when the stress is increased. High-strength concrete has a more linear relation between stress and strain than ordinary concretes. The proportionality of high-strength concrete is due to a decreased development of cracks in the stress range less than 70 % of the compressive strength. High-strength-concrete is achieved by, among other things, reducing the water/cement ratio which has an influence of the development of cracks.

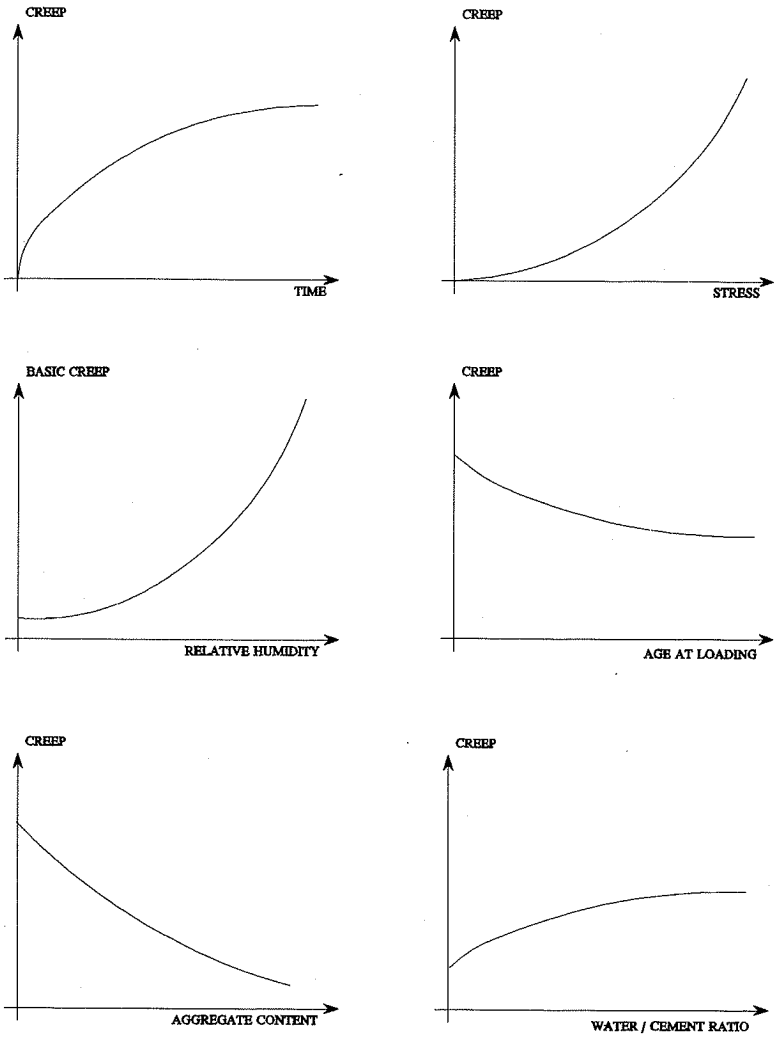

Fig. 1.2 Schematic illustration of the relationship between creep and some of the factors influencing creep.

After a period of 4 to 16 hours after the concrete has been cast, the hydration of the cement starts. The hydration of the cement reduces the amount of evaporable water in the concrete and increases the compressive and tensile strength. Usually the mechanical properties are determined after 28 days of curing. The concrete continues to hydrate after 28 days but at a decreasing rate. If a load is applied to the concrete during the period of hydration, then creep is related to the development of strength during the creep and hydration period. The stress/strength ratio is decreased by the development of the strength. The strength development is related to the water/cement ratio.

This brief review of the most significant factors influencing creep illustrates that creep is related to the water/cement ratio.
The fact that the 8 factors are related by at least one common factor indicates that it is more or less impossible to investigate the influence of just one factor, because it is impossible to change one factor without affecting at least one or two other factors.
Despite the above mentioned difficulty, it is possible to underline some of the effects which are observed to be related to the listed number of factors influencing creep. The influence of most of the factors is similar to the effects on shrinkage.

The mechanical properties, such as modulus of elasticity, porosity and absorption of the aggregate have a documented effect on concrete creep. Aggregates in normal-weight concrete do not usually exhibit creep or shrinkage, nor do they adsorb water from the cement paste. As mentioned, creep is related to the cement paste, the aggregate restrain creep and as the cement paste creeps the stress of the aggregates are increased.
The difference between the mechanical properties of the cement paste and the mechanical properties of the aggregate has an influence on the amount of the stress redistribution between paste and aggregate. The larger the difference between the cement paste and the aggregate the more significant is the stress redistribution.
The effect of the aggregate/paste ratio is quite similar to the effect on shrinkage. {1.2} is an extended relation between aggregate content and concrete creep. {1.2} accounts for the unhydrated cement which acts like fine aggregate.

$$\varepsilon_{cr,concrete} = (1 - g - u)^a \cdot \varepsilon_{cr,paste} \qquad \{1.2\}$$

$\epsilon_{cr,concrete}$	Creep of concrete
g	Aggregate content
u	Unhydrated cement

$\epsilon_{cr,paste}$	Creep of neat cement paste
a	1-1.37 according to Neville [83.7] but is dependent on the mechanical properties of the aggregate.

The influence of the relative humidity is two sided. Shrinkage does not appear in hydrostatic equilibrium. Creep appears during a period of hydrostatic equilibrium and is reckoned as basic creep. For a concrete which is in hydrostatic equilibrium, creep increases when it is subjected to a higher relative humidity. Concrete usually creeps during a period of drying when it is not in hydrostatic equilibrium. Creep is usually increased when the relative humidity is decreasing and the concrete is not in hydrostatic equilibrium.

Some of the non-linearity of the stress-strain relationship is due to creep during the application of the load. A significant amount of the non-linearity is due to deformations in existing cracks or development of new cracks. The influence of the cracks is enhanced by creep. The cracks contribute to the total creep in the order of 10-25 % of the non-crack creep.

The sooner a load is applied to the concrete during hydration the larger creep is observed. If a concrete is loaded after complete hydration and the concrete is in hydrostatic equilibrium, then no creep appears in the concrete.

1.3 Theories and mechanisms of shrinkage

Shrinkage can be divided into two fundamentally different groups:

Chemical shrinkage
Physical shrinkage

The chemical shrinkage can be subdivided into carbonation and hydration. Both chemical shrinkage and physical shrinkage is related to water inside and outside of the concrete.
The products of hydration caused by the hydration between the cement and the water has a smaller volume than the sum of the volume of the cement and the water used in the chemical reaction. The reduction of volume in relation to the amount of cement is in the order of magnitude of 25 % [91.6]. This chemical shrinkage causes the porosity of the concrete and does not cause an exterior shrinkage of any significance.
The chemical shrinkage is related to the water/cement ratio. Concretes with a water/cement

ratio less than 0.42 will to some extent use not only capillary water but also some of the gelwater for hydration.

As long as just capillary water is used for the hydration, then chemical shrinkage, as described, takes place and causes a negligible external shrinkage. During hydration based upon capillary water the relative humidity inside the concrete is close to 100 %.

Use of gelwater for hydration decrease the internal relative humidity and cause a significant shrinkage named selfdesiccation shrinkage. Selfdesiccation shrinkage is caused by a chemical action which causes a physical reaction which is similar to drying shrinkage which is a physical shrinkage. The distribution of the concrete volume in relation to the degree of hydration is illustrated in Fig. 1.3.

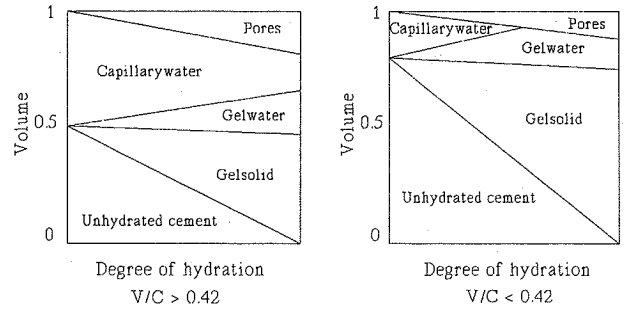

Fig. 1.3 The distribution of the concrete volume in proportion to the degree of hydration. [85.8]

Drying shrinkage is caused by a loss of water from the concrete. The volume of the evaporated water is not equivalent to the shrinkage volume [83.7]. The loss of water cause a change in :

1 The colloidal stress
2 Adsorbed water
3 Capillary stress

The cementgel is a colloid i.e. a system of particles with a large surface/volume ratio. The surface stress of a colloid particle is decreased as the relative humidity is increased and water is adsorbed to the surface of the particles. A decrease of the surface stress of the colloid particles causes an expansion of the particles. The relation between volume change of colloid stress and relative humidity is illustrated in Fig. 1.4-1.

The average distance between the gelparticles is 15-20 Å. Particles which are so close together attract each other by van der Waals' forces.
Water adsorbed to the surface of the gelparticles increases the distance between the gelparticles. The more layers of water adsorbed to the gelparticles the more the gelparticles are separated. As the distance between the gelparticles is increased, the van der Waals' forces are decreased. The relation between volume change of adsorbed water and relative humidity is illustrated in Fig. 1.4-II.

In a saturated cementgel there are no *menisci*. As the relative humidity is decreased menisci appear in the capillary pores. The menisci cause tensile stresses in the capillary water which remove adsorbed water from the cementgel. As the water evaporates the menisci are broken and the tensile stresses are relieved and the adsorbed water returns to the surface of the gelparticles. At relative humidities less than approximately 45 % there are no capillary stresses. The relation between volume change due to capillary stress and relative humidity is illustrated in Fig. 1.4-III.

The three mechanisms act at the same time and cause a shrinkage/relative humidity relationship which has a typical S-shape caused by the effect of the capillary stress. The relationship of the three shrinkage mechanisms acting at the same time is illustrated in Fig. 1.4.
It must be emphasized that only the gelwater participates in shrinkage. Evaporation of capillary water alters the internal water pressure which affects the gelwater.

The shrinkage mechanisms mentioned concern neat cement paste. Concrete shrinkage is less than shrinkage of neat cement paste, as mentioned . The aggregate of the concrete restrain the shrinkage of the neat cement paste. Concrete is in fact a composite material and a composite model can be considered.
The composite model consist of an coarse aggregate sphere surrounded by a matrix sphere. The model is treated as a linear elastic problem and a general solution can be determined. The main result of the model is that tensile stresses can be determined and it can be proven that the tensile stresses can exceed the tensile strength of the paste.
Another important result of the composite model is that the relation between concrete shrinkage ($\epsilon_{sh,c}$), shrinkage of the cement paste ($\epsilon_{sh,p}$) and the aggregate content (g) can be determined as {1.3} for $E_g/E_p > 10$. E_g being the elastic modulus of the coarse aggregate and E_p the elastic modulus of the cement paste.

$$\varepsilon_{sh,concrete} = (1 - g)^2 \cdot \varepsilon_{sh,paste} \qquad \{1.3\}$$

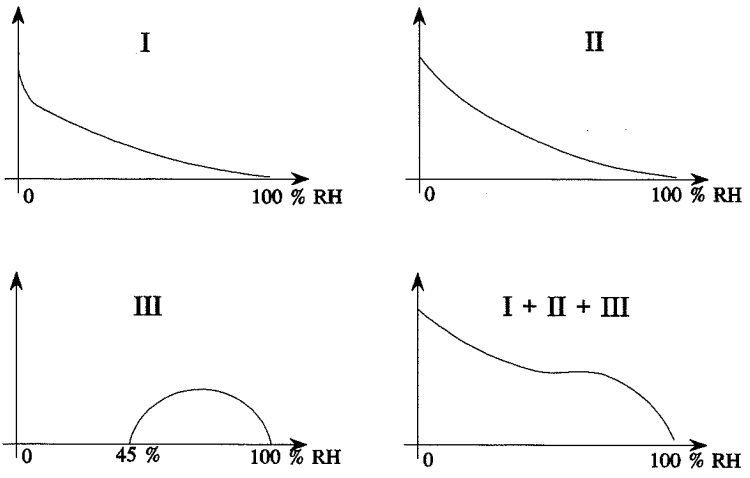

[Unpublished notes by T.C. Hansen]

Fig. 1.4 Schematic illustration of the three shrinkage mechanisms. I - colloidal stress; II - Adsorbed water; III - capillary stress. The illustration concerns shrinkage after hydrostatic equilibrium has been reached.

{1.3} is quite similar to {1.1} except for the exponent. The results mentioned did not consider creep of the paste.

The cracks caused by the restraint of the aggregate appear as a net pattern of microcracks

Another significant kind of restraint causing shrinkage cracks is due to surface drying and appears in a cement paste specimen too.

As the water evaporates from the surface of a specimen the cementpaste shrinks faster at the surface of the specimen than in the core of the specimen. The delayed shrinkage in the core cause a state of tensile stresses at the surface and compression stresses in the core of the drying specimen. The delay in the shrinkage rate is dependent on the porosity of the paste. A large selfdesiccation can decrease the differential shrinkage between the surface and the core.

In Fig. 1.5 the consequence of the differential shrinkage is illustrated. The cylindrical specimen shrinks from the original position A to position B. The restraint of the core causes a curvature of the plane circular ends of the cylindrical specimen considered.

If the tensile strength is exceeded at the surface the concrete cracks and the tensile stresses are

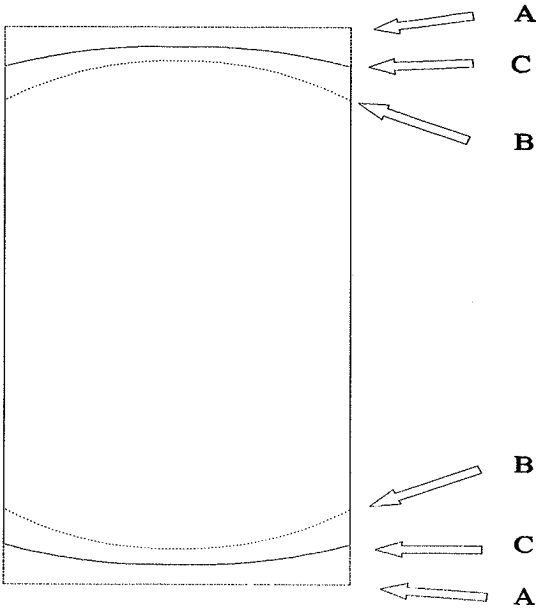

Fig. 1.5 Deformation due to differential shrinkage at the specimen surface and the specimen core.

relieved at the surface. The specimen expands to position C after cracking. The surface cracks appear as microcracks in the first stage of drying. After a period of drying and subsequent cracking macrocracks appear at the surface.

In Fig. 1.6 two macrocracks patterns caused by surface drying are illustrated. Crack pattern III in Fig. 1.6 is due to swelling or due to selfdesiccation of water stored specimens.

The restraint of the core due to surface drying is more significant for neat cement paste than for concrete, as the shrinkage and subsequently the differential shrinkage in a concrete specimen is decreased by the aggregate restraint. While the restraint of the aggregate is independent on the specimen size and shape, the restraint by the specimen core is dependent on the mechanical properties of the concrete components and the specimen size. The restraint of the core is relieved by creep.

The consequence of the surface drying is that a surface measurement does not reveal the "true" shrinkage. As a matter of fact, a surface/internal measurement of an ideal specimen drying uniformly all over does not reveal the true concrete shrinkage either, as the aggregate

causes creep in the paste too.

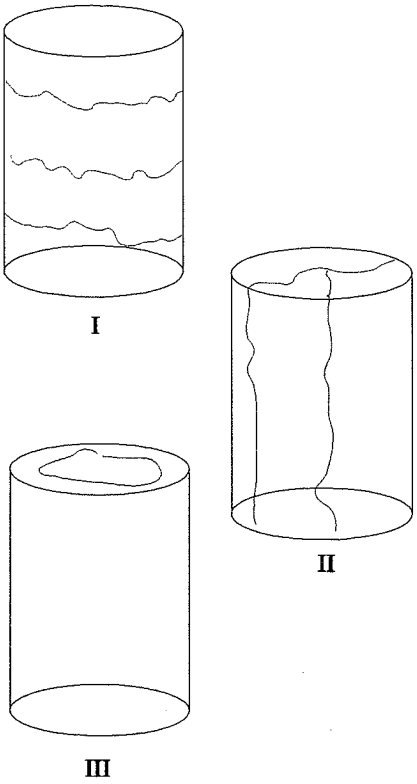

Fig. 1.6 Macrocrack patterns due to differential shrinkage.

1.4 Mechanism and theories of creep

While the mechanisms of shrinkage are commonly accepted, the theories of creep are more numerous [83.7]. The large number of theories is a consequence of the fact that none of the proposed theories can explain all creep phenomenons.

A combination of the theories would be able to explain a large number of the observations. The combination of theories indicates that more than one mechanism is the cause of creep.

In the subsequent 4 theories are described briefly. The 4 theories are *plastic flow* which treat concrete like a metal, *visco-elasticity* which treat concrete as i highly viscous fluid. Visco-elasticity is often used by means of rheological models which are suited to fit test data. The third theory is *seepage theory* and is the one which has gained most support among the researchers who deal with creep and shrinkage. In addition to the 3 theories, *microcracks* contribute to creep but do not explain the rheological behavior of creep.

1.4.1 Plastic flow

Plastic flow as crystalline slip has been suggested to be the cause of creep. Plastic flow is caused by a slip in a plane of maximum shear stress. The presence of water acts like a lubricant and makes flow easier. A slip in a plane of maximum shear does not result in a volume change and concrete creep actually exhibits a volumetric decrease. In relation to concrete, plastic flow is more like a conception than an explanation.

1.4.2 Viscous flow

Viscous flow has been suggested as a concrete creep mechanism. The cement paste is considered as a fluid with a high viscosity. As the paste deforms in a linear time-dependent rate the stress at the aggregate is increased. The deformation of a viscous fluid is proportional to the applied stress and as the aggregate takes over, the deformation rate decrease and is reckoned as the decreasing creep rate.

Like plastic flow viscous flow requires a constant volume and viscous flow furthermore requires a proportionality between stress and strain which is not the case with concrete. Concrete has a proportionality limit in the range of 30-50 % of the strength. However the lack of proportionality does not exclude viscous flow as a creep mechanism, as the proportionality limit is believed to be due to microcracking.

1.4.3 Seepage theory

The seepage theory has already been described, as the shrinkage mechanism described is identical to the seepage theory. According to the seepage theory the gelwater is the water causing creep and shrinkage. The gelwater in a concrete specimen is in a state of equilibrium

vapor pressure. As an external load is applied to the concrete specimen the pressure of the gelwater is altered. To obtain equilibrium again, the gelwater is reorganized. The reorganization of the gelwater affects the colloidal stresses and the van der Waals' forces. Equilibrium is obtained by a seepage of gelwater inside the cement gel.

The rate of the seepage is dependent on how dense the cement paste is. The more dense the paste is, the slower seepage. The seepage is also dependent on how far the gel water has to travel to obtain equilibrium. The gelwater probably becomes capillary water and has to migrate to a capillary pore to establish equilibrium during the time of external loading. A removal of the external load lowers the pressure on the gelwater and the original equilibrium is established. Creep recovery tests show that the original size of the specimen is seldom reached, except for unique conditions. The reason why the original position is never reached again, is probably due to formation of new gel during the load period. The new gel is in a state of equilibrium while the external load is applied, but is not in a state of equilibrium after unloading and in fact counteracts the original gels attempt to establish equilibrium.

One would believe that if the gelwater slowly is squeezed out of the gelpores and the capillary water evaporates then a larger weightloss should be determined during creep than during shrinkage. Tests conducted to confirm this assumption have not proven this to be true. Creep specimens evaporate the same amount of water as shrinkage specimens. It has been suggested that the test equipment was not accurate enough to measure this small amount of water. Even though the difference has not been proven, it does not exclude seepage theory as a mechanism of creep, as internal seepage still may occur.

Never the less, the presence of evaporable water is a prerequisite of creep and shrinkage. As the mechanism of creep according to the seepage theory is similar to the mechanism of shrinkage, the concept "stress-induced shrinkage" has been caused by some authors.

1.4.4 Microcracking

The presence and development of microcracks in the concrete has a significant influence on the stress-strain relationship of concrete and contributes to creep. A comparison of the stress-strain relationship of partly the aggregate and partly the cement paste of which a certain concrete is composed, reveals that the aggregate and the cement paste exhibit linearity, while the composite material (concrete) exhibits non-linearity. According to the composite theory, a composite material composed by two linear materials is also a linear material. The

discrepancy is due to microcracks at the interface of the coarse aggregate and the mortar or cracks in the mortar.

Two different kinds of microcracks can be identified in concrete. Bond cracks or mortar cracks. Bond cracks are cracks at the interface of the coarse aggregate and the mortar. Mortar cracks are obviously cracks in the mortar.

Some microcracks are developed in the concrete in the early ages by plastic shrinkage and appear usually as bond cracks. Later on cracks can form because of shrinkage in general and are caused by the restraint of the aggregate and/or surface drying, as mentioned in section 1.3. Shrinkage cracks can appear as bond cracks and/or mortar cracks. A more or less well developed crack pattern exists in all concrete before an external load is applied to a concrete specimen.

As an external load is applied to the concrete, the aggregate and the mortar deform and exhibit lateral strain according to their respective Poisson ratios. The difference in lateral strain causes an increase of existing shrinkage cracks or formation of new cracks. The larger the difference between the Poisson ratio of the mortar and the aggregate, the more cracks are developed.
A high-strength concrete mortar does not differ as much from the aggregate as a low-strength concrete mortar, as far as the stress-strain relationship is concerned, and as a corollary less cracks are developed in a high-strength-concrete as compared to a low-strength-concrete. High-strength-concrete is a more linear material than low-strength-concrete because of the low crack development rate, this has been proven by e.g. Carrasquillo [80.2].

At a stress/strength ratio of 30-40 % the microcracks do have a significant influence on the stress-strain relationship. At the same stress/strength level concrete ceases to be linear due to the microcracks. At a stress/strength level of 75-85 % the crack growth rate is accelerating and an sustained external force at this load-level will cause failure. This failure is known as creep rupture, static fatigue or long-life strength.

Microcracks can be caused by shrinkage or thermal stress before a sustained load is applied to the concrete and cracks can be developed while the load is increased to a wanted load-level. A microcrack develops with a certain rate in relation to the load, the loading rate and the material in which the crack develops. The cracks are probably still in progress after the load increase is ceased, and the wanted load-level has been reached, and therefore cause creep. After a relatively short period of time the cracks become stable and microcracks do not

contribute to creep anymore. Microcracks are still developed by shrinkage and thermal stresses during the load period. Shrinkage and thermal cracks are developed more easily during the load period. At the wanted load-level and with the cracks in a stable condition, just a small increase of the stresses at a crack tip will cause a progress of the crack. Hence, shrinkage and thermal stresses will cause more microcracks for small shrinkage or thermal strains. This mechanism probably contributes significantly to drying creep. In relation to "Stress-induced shrinkage" this mechanism is "Shrinkage-induced stress" or "Shrinkage-induced creep". The

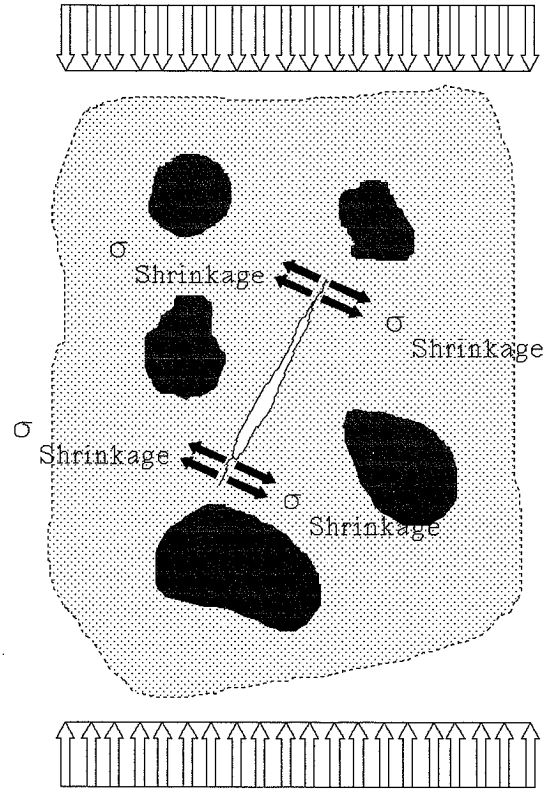

Fig. 1.7 Development of microcracks caused by shrinkage

mechanism is illustrated in Fig. 1.7. Tests performed by Ali S. Ngab [80.1] support this hypothesis as illustrated in Fig. 1.8. Fig. 1.8 illustrates an increase in bond crack length of unsealed normal-strength-concrete during creep. Sealed specimens do not show any increase

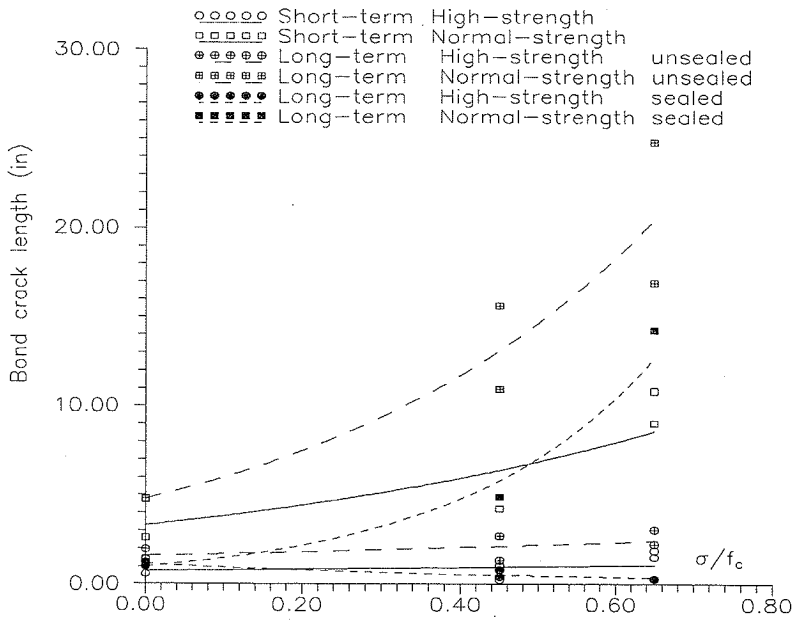

Fig. 1.8 Shrinkage-induced cracks. Ali S. Ngab [80.1]

in the bond crack length. As known, unsealed specimens shrink more than sealed specimens and according to the above hypothesis, this causes more cracks during loading.

High-strength concrete exhibits no difference between sealed and unsealed specimens, which corresponds to the lack of drying shrinkage and drying creep.

A corollary of the hypothesis is that no drying creep is supposed to occur when drying shrinkage ceases.

Anders Nielsen [72.1] has emphasized that the increase of stresses caused by surface drying acts like an external load applied to the specimen core and causes an additional creep corresponding to drying creep. Drying creep may be caused by lack of surface cracks in the creep specimen. Fig. 1.5 illustrates that a surface crack caused by shrinkage results in a

measured shrinkage which is too small when compared to the uncracked surface shrinkage. While the creep specimen is loaded in compression, tensile stresses at the surface are neutralized by the compression and no surface cracks will appear. When no cracks appear, the surface shrinkage is larger and the values of shrinkage which are withdrawn according to the definition of creep are too small. Drying creep is overestimated in relation to this mechanism.

Kesler & Ali [64.4] {1.4} and Neville [69.2] {1.6} have proposed empirical formulas relating creep to shrinkage. These formulas are not based upon the assumption that microcracks and shrinkage are related.

$$\varepsilon_{dc} = \sigma \beta \varepsilon_{sh} (a + b/t) \qquad \{1.4\}$$

$$\beta = \frac{(1 - Va - Vuc)^2}{Vhc^2} \qquad \{1.5\}$$

ϵ_{dc}	Drying creep
ϵ_{sh}	Shrinkage strain
σ	Applied stress
ß	Gel compliance factor
a,b	Constants
t	Time
Vhc	Volume concentration of hydrated cement
Va	Volume concentration of aggregate
Vuc	Volume concentration of unhydrated cement

$$\varepsilon_c = \frac{\sigma}{f_c} k \times (a + b/t) (1/Q + \varepsilon_{sh}) \qquad \{1.6\}$$

ϵ_c	Creep
ϵ_{sh}	Shrinkage strain
σ	Applied stress
k	34000 psi
a,b	Constants
t	Time

x	Gel/space ratio
Q	Constant

Z.P. Bazant & J-K. Kim [92.2] have proposed an equation {1.7} related to {1.4}.

$$c_d = q_5 \cdot k_h \cdot \varepsilon_{sh\infty} \cdot f(t) \qquad \{1.7\}$$

c_d	Drying creep
q_5	Empirical constant related to the compressive strength
k_h	Factor related to the relative humidity of the environment and the humidity of the specimen core
$\epsilon_{sh\infty}$	Final shrinkage
f(t)	Time function

The symbols in {1.4} to {1.7} are named in relation to the respective references.

2 DEFINITION OF TERMS AND CLASSIFICATION

In the following discussion and analysis of the test results a number of terms are used. Some of the terms are based upon a direct measurement and are defined in the test report, as well as mentioned here. For further analysis a larger number of terms has to be introduced and these are defined in this chapter.
The concretes are classified into 5 groups based upon the compressive strength.

2.1 Definition of terms

Shrinkage strain (ϵ_{sh}) is a direct measurement. The shrinkage strain is the time-dependent deformation observed at an unloaded specimen. The specimen can be exposed to drying or the specimen can be sealed.
The shrinkage strain observed on a specimen exposed to drying is denoted the total shrinkage ($\epsilon_{sh,t}$) and the shrinkage strain observed on a sealed specimen is denoted basic shrinkage ($\epsilon_{sh,b}$). Basic shrinkage is also known as autogenous shrinkage and/or chemical shrinkage.
The drying shrinkage ($\epsilon_{sh,d}$) can not be measured directly, however, it can be determined as the difference between a specimen exposed to drying and a sealed specimen. The drying shrinkage can be expressed as in {2.1}.

$$\varepsilon_{sh,d} = \varepsilon_{sh,t} - \varepsilon_{sh,b} \qquad \{2.1\}$$

The basic shrinkage is often assumed to be equal zero which can lead to contradicting results (see later). The shrinkage strains are illustrated in Fig. 2.1.

The initial strain (ϵ_0) is the strain observed at the very minute the concrete specimen has been loaded to the wanted load-level (σ). The secant modulus corresponds to the initial strain and the wanted load-level as in {2.2}.

$$E_s = \frac{\sigma}{\varepsilon_0} \qquad \{2.2\}$$

The total strain (ϵ_{total}) is the strain of a loaded specimen. The total strain is a direct measurement. The loaded specimen can either be exposed to drying or be sealed . The total strain of a specimen exposed to drying is denoted $\epsilon_{total,t}$ and the total strain of a sealed specimen

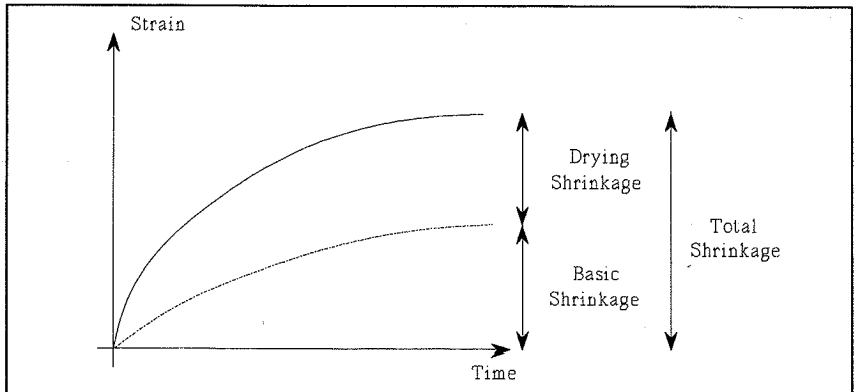

Fig. 2.1 Shrinkage strains

is denoted $\epsilon_{total,b}$.

The creep strain (ϵ_{cr}) is the additional strain observed with respect to the initial strain and the shrinkage strain. The creep strain of a specimen exposed to drying is denoted $\epsilon_{cr,t}$. The creep strain of a sealed specimen is denoted $\epsilon_{cr,b}$ and is known as basic creep. The creep strains are indirectly determined by {2.3} and {2.4}.

$$\varepsilon_{cr,t} = \varepsilon_{total,t} - \varepsilon_0 - \varepsilon_{sh,t} \qquad \{2.3\}$$

$$\varepsilon_{cr,b} = \varepsilon_{total,b} - \varepsilon_0 - \varepsilon_{sh,b} \qquad \{2.4\}$$

The drying creep ($\epsilon_{cr,d}$) is like the drying shrinkage indirectly determined. The drying creep is the additional creep strain observed between a sealed specimen and a specimen exposed to drying during the loadperiod. The drying creep is defined in {2.5}.

$$\varepsilon_{cr,d} = \varepsilon_{cr,t} - \varepsilon_{cr,b} \qquad \{2.5\}$$

{2.5} can be expressed in terms of {2.3} and {2.4}

$$\varepsilon_{cr,d} = \varepsilon_{total,t} - \varepsilon_{total,b} - \varepsilon_{sh,t} + \varepsilon_{sh,b} \qquad \{2.6\}$$

The expression {2.6} shows that if the basic shrinkage ($\epsilon_{sh,b}$) is incorrectly assumed to be zero, then the drying creep will be underestimated.

A higher compressive strength gives less drying shrinkage and more basic shrinkage. This fact emphasizes the necessity of measuring the basic shrinkage.

Concrete is not a linear visco-elastic material and therefore the creep coefficient (φ) and the specific creep (c) are defined in order to analyze and compare results from different concretes. The creep coefficient is defined as the ratio between the creep strain and the initial strain {2.7}.

$$\varphi = \frac{\varepsilon_{cr}}{\varepsilon_0} \qquad \{2.7\}$$

Anders Nielsen |72.1| has emphasized that φ is dependent on the way the initial strain has been determined. The creep strain is related to the initial strain by {2.3} or {2.4} which leads to the relative deviation of the creep coefficient {2.8}.

$$\frac{\Delta\varphi}{\varphi} = -\frac{1+\varphi}{\varphi} \cdot \frac{\alpha}{1+\alpha} \quad ; \quad \alpha = \frac{\Delta\,\varepsilon_0}{\varepsilon_0} \qquad \{2.8\}$$

In Fig. 2.2 the problem is illustrated. On the basis of {2.8}, Anders Nielsen has pointed out the difficulty of separating ϵ_{cr} and ϵ_0. Theoretically the distinction between ϵ_{cr} and ϵ_0 is rather exact, however, based upon experimental results it is more or less impossible to determine the exact value of ϵ_0. The conclusion of Anders Nielsens analysis is that one must be cautious when comparing different experimental results with small values of φ.

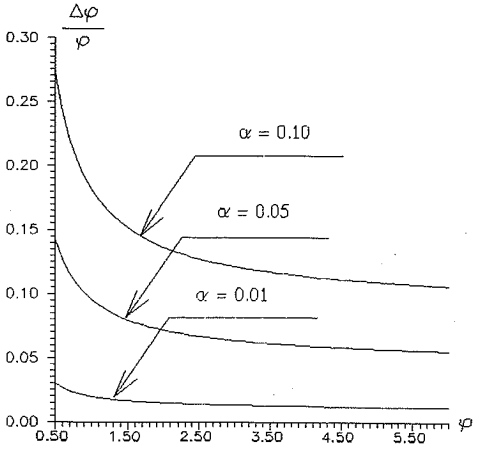

Fig. 2.2 Deviation of the creep coefficient. |72.1|

Fig. 2.3 and Fig. 2.4 illustrate the problem for both a hydraulic loading frame and a dead-load lever arm creep rig. In the figures c is $1 \pm \alpha$.

In addition to the difficulty of separating ϵ_{cr} and ϵ_0, ϵ_0 is dependent on the loading rate.

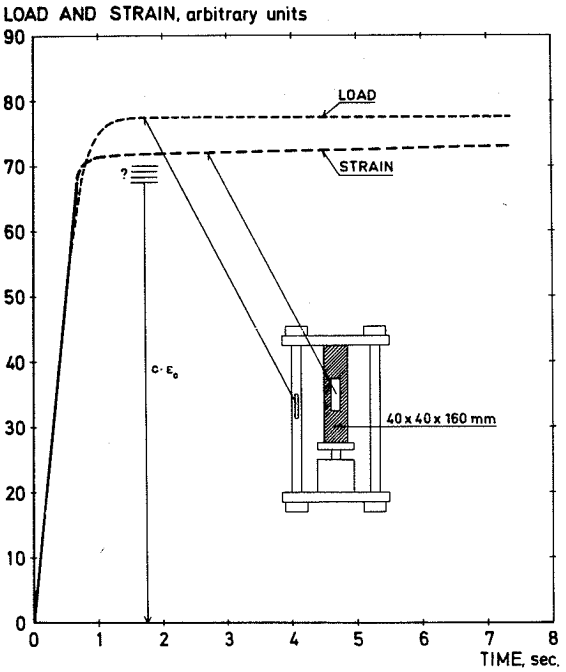

Fig. 2.3 Load and strain versus time during loading in a hydraulic load frame. [72.1]

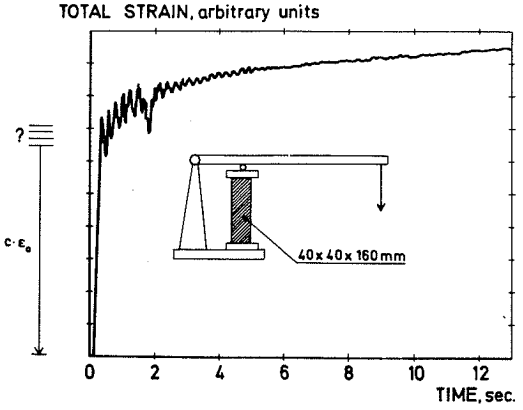

Fig. 2.4 Strain versus time in a dead-load lever arm creep rig. [72.1]

When analyzing High-Strength-Concrete it is important to keep these problems in mind, as High-Strength-Concrete exhibits small values of φ.

Another term used for analyzing creep is the specific creep (c), defined as the creep per unit stress {2.9}

$$c = \frac{\varepsilon_{cr}}{\sigma} = \frac{\varepsilon_{cr}}{E_s\ \varepsilon_0} = \frac{\varphi}{E_s} \qquad \{2.9\}$$

The specific creep suffers from the same uncertainty as the creep coefficient, which is obvious in {2.9}. The secant-modulus (E_s) is load-dependent and the specific creep is not just another way to express the creep coefficient.

Some terms related to the stages of creep are presented in Fig. 2.5. The primary and secondary creep are usually observed. The tertiary stage of creep does not take place unless static-fatigue failure occur. The "true" elastic strain is due to the development of stiffness and strength.

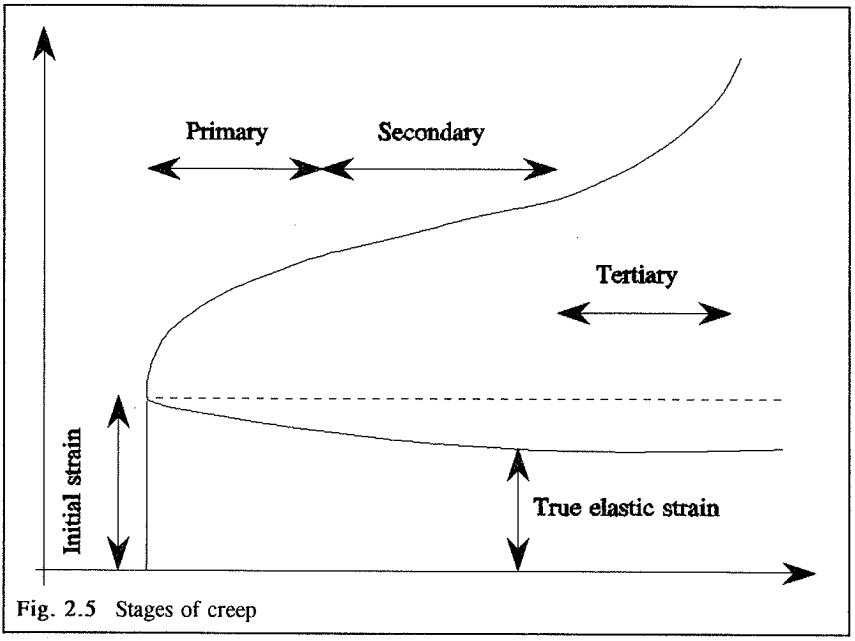

Fig. 2.5 Stages of creep

2.2 Classification

The designer often identifies a concrete by the concretes uniaxial compressive strength. The compressive strength is obviously not the cause of the creep and shrinkage. The compressive strength is a result of e.g. water/cement-ratio, amount of evaporable water, porosity etc., etc. Never the less, the compressive strength is easy to determine and is often the only parameter prescribed for structural use.

Based upon the above considerations, the concretes in this investigation are classified by means of the compressive strength into 5 groups as illustrated in Table 2.1.

Table 2.1 *Classification according to the compressive strength*

Classification	Shortening	Compressive strength
Very-Low-Strength-Concrete	VLSC	0-10
Low-Strength-Concrete	LSC	10-30
Normal-Strength-Concrete	NSC	30-60
High-Strength-Concrete	HSC	60-85
Very-High-Strength-Concrete	VHSC	85-110

3 GENERAL OBSERVATIONS OF COMMON MECHANICAL PROPERTIES

In this section the relations between the compressive strength, the elastic modulus, the dynamic modulus and the water/cement ratio are discussed and analyzed.
As pointed out in the introduction most mechanical properties of concrete can be related to the water/cement ratio. The use of different kinds of pozzolans affects the water/cement ratio. Comparing different mechanical properties in relation to the water/cement ratio of different kinds of concretes with and without pozzolans may cause strange and unpredictable relations. Using the water/binder ratio may not improve the relations because the activity factor may be different for different mechanical properties.
To avoid any misinterpretations, just the water/binder ratio without any activity factors is considered in the analysis of the relations between mechanical properties and the water/binder ratio.

3.1 The relation between the compressive strength and the water/binder ratio

The designer often only knows the mechanical properties of a concrete in relation to the uniaxial compressive strength (f_c). Comparing mechanical properties in relation to the compressive strength requires that the concretes are comparable in this way i.e. the aggregate must be the same and the aggregate content must be the same and so on. As an example from this investigation of the mechanical properties of mix no. 5 and 6, the compressive strength after 29 days of curing is equal for the concretes and their respective pastes, but the elastic modulus varies and the shrinkage and creep show a quite different behavior.
For structural design, the compressive strength is often the only mechanical property required. For quality control the compressive strength is a convenient parameter because the compressive strength is easily determined.
In the subsequent sections most mechanical properties are analyzed in relation to the compressive strength. The correlation between the compressive strength and the water/binder ratio is illustrated in Fig. 3.1.
The relation between the compressive strength and the water/binder ratio is good even though no distinction has been made as to whether microsilica fume or fly ash has been used or not. The intimate relationship illustrated in Fig. 3.1 reveals that referring to the compressive strength or the water/binder ratio is just a matter of affinity.
It must be emphasized that this affinity is valid only for the concretes considered in Fig. 3.1. Discrepancy between other investigations may occur when comparisons are performed in relation to the compressive strength. The discrepancies may be due to different aggregate

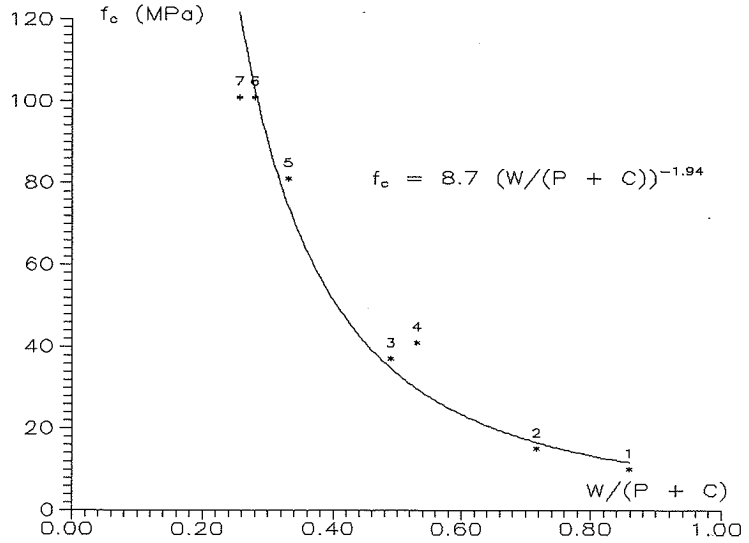

Fig. 3.1 The uniaxial compressive strength in relation to the water/binder ratio. The numbers refer to the mix number. The test values are mean values of the whole test series.

content and the use of pozzolans.

3.2 The relation between the compressive strength and the modulus of elasticity.

Most structural codes consider the elastic modulus of concrete as a mechanical property uniquely related to the compressive strength.

However the relationship between the elastic modulus and the compressive strength is dependent on the moisture conditions of the concrete.

A concrete has a higher E-modulus when it is wet than when it is dry. On the contrary, the strength is lower for the same concrete when it is wet than when it is dry, see section 7.

The mechanical properties of the aggregate and the aggregate content affect the elastic modulus more significantly than these properties affect the compressive strength.

In Fig. 3.2 the relations between the elastic secant modulus at the age of 29 days ($E_{\infty 0}$) and the compressive strength (f_c) at the same age are depicted. The σ/f_c-ratio is 1/3. Regarding

moisture content, the specimens have surface dried 2 days after 27 days of water-curing.

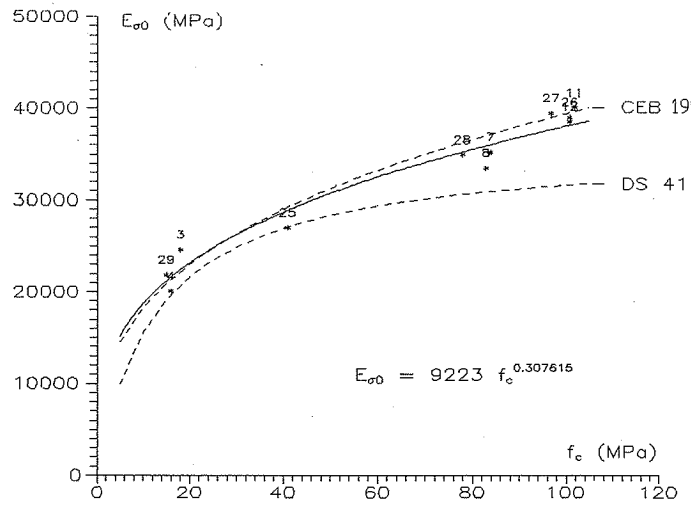

Fig. 3.2 Relation between the elastic modulus and the compressive strength of the test specimens. The danish code DS 411 and CEB-FIP modelcode 1990 are also illustrated.

The test results are compared to the CEB-FIP modelcode 1990's [90.7] assumption of the relation between elastic secant modulus and compressive strength {3.1} and the same assumption of the danish code 411 [84.5] {3.2}.

$$E_{\sigma 0} = 0.85 \cdot 2.15 \cdot 10^4 \left(\frac{f_c}{10} \right)^{1/3} = 8483 \cdot f_c^{1/3} \qquad \{3.1\}$$

$$E_{\sigma 0} = 0.7 \cdot 51000 \frac{f_c}{f_c + 13} \qquad \{3.2\}$$

f_c in MPa. The danish code is only valid for compressive strength less than 50 MPa.
In Fig. 3.2 a fair correlation can be observed between DS 411 and the test results in the range of 10 - 50 MPa.
The correlation between the CEB model and the test results is quite good.

The influence of the aggregate may cause a small discrepancy. The aggregate content of the

LSC is 0.84 and the aggregate content of the VHSC is 0.76. As mentioned, a lowered aggregate content will decrease the elastic modulus according to the composite theory. Composite models proposed by Hirsch [62.1], Dougill [62.2] and Counto [64.3] indicate that a change of the aggregate content by 0.08 causes a change of E_{c0} by 4400 MPa, assuming that the aggregate modulus is E_a = 50000 MPa and that the modulus of the paste is E_p = 25000 MPa.
The CEB model does not take account of the aggregate content, which probably would cause a better correlation between the test results and the model, as the CEB values would be decreased in the high strength region and increased in the low strength region.

3.3 The relation between dynamic modulus and elastic modulus

The dynamic modulus of concrete is dependent on the properties of the aggregate, the aggregate content and the moisture conditions in the concrete. The dynamic modulus is also very sensitive to cracks which are perpendicular to the pulse direction.
In Fig. 3.3 the relation between the dynamic modulus and the elastic modulus is illustrated. The dynamic modulus is determined for Ø100 x 200 cylinders, which are assumed to be long slender specimens. Hence the dynamic modulus can be determined by {3.3}.

$$E_{dyn} = \left(\frac{l}{t} \right)^2 \cdot \rho \qquad \{3.3\}$$

l	length
t	pulse time
ρ	density of the concrete

If the specimen is not a long slender specimen, the dynamic modulus is affected by the Poisson ratio (ν) as in {3.4}.

$$E_{dyn} = \left(\frac{l}{t} \right)^2 \cdot \rho \cdot F(\nu) \qquad \{3.4\}$$

$$F(\nu) = \frac{(1 + \nu)(1 - 2\nu)}{1 - \nu} \qquad \{3.5\}$$

$$0 \leq F(\nu) \leq 1 \qquad \{3.6\}$$

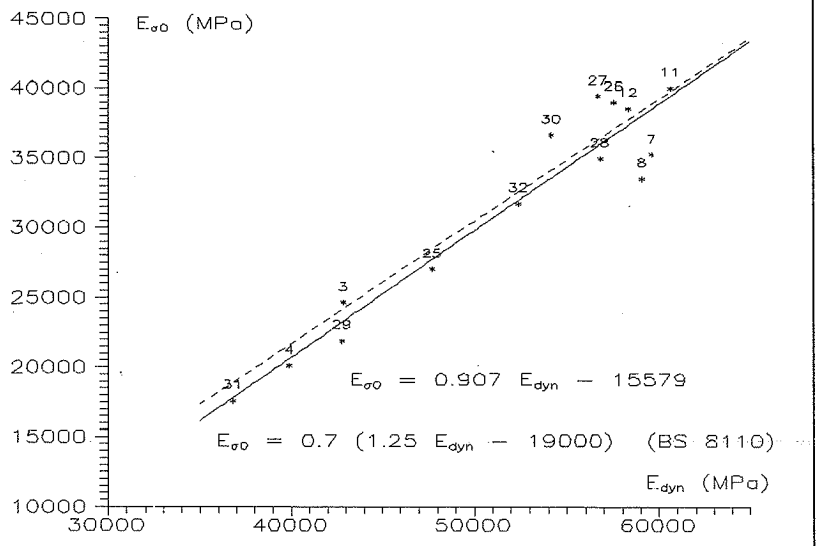

Fig. 3.3 The relationship between the dynamic modulus and the elastic modulus is illustrated by a solid line. The assumption of British Standard 8110 is illustrated by a dashed line.

British standard BS 8110 assumes {3.7} as the relationship between the dynamic modulus and the elastic modulus.

$$E_{\sigma 0} = 1.25 \cdot E_{dyn} - 19000 \quad (\ MPa\ ) \qquad \{3.7\}$$

$E_{\sigma 0}$ in {3.7} is the initial tangent modulus. In Fig. 3.3 is {3.7} multiplied by 0.7. A quite good correlation between the dynamic modulus and the elastic modulus is then achieved.
If the specimens can not be considered as long slender specimens, then the poisson ratio has to be accounted for. If $F(\nu) = 0.7$ in {3.5}, then the poisson ratio is less than 0.319 for the tested concretes.

3.4 Conclusions

1. During further analysis in this report the mechanical properties can be analyzed in relation to the compressive strength as well as the water/binder ratio, as the two parameters are well correlated.

2. With regards to the relation between elastic modulus and compressive strength the concretes investigated in this report correspond to the empirical CEB-FIP model code 1990. The test data exhibit the same trend as the CEB-FIP modelcode.

3. Existing concrete models for E_{dyn} and the relation between E_c, f_c can be used in relation to concretes with compressive strength up to 100 MPa.

4 SHRINKAGE OF CONCRETE

In this section the concrete shrinkage determined in the test report is analyzed.
The shrinkage is analyzed in relation to the compressive strength.
The CEB-FIP modelcode 1990 is considered in order to evaluate the test results, and the model. The CEB-FIP modelcode 1990 is an emperical approach calibrated to test data.
The influence of carbonation, selfdesiccation and the aggregate content are discussed too.

4.1 Experimental results

In Fig. 4.1 the shrinkage of the 7 different concretes exposed to drying and the 3 sealed concretes is presented. The shrinkage illustrated in Fig. 4.1 is the shrinkage after 27 days of water curing and 2 days of air curing. It can be seen from Fig. 4.1 that all shrinkage curves follow the same trend/shape and do not cross one another in any significant way except of crossings related to test scatter. The 3 sealed test series exhibit almost the same shrinkage, although the strength range is from 16 to 101 MPa.
In Fig. 4.2 the shrinkage strains of mix no. 2, 5 and 6 (LSC,HSC and VHSC) are illustrated. The shrinkage curves represent the shrinkage after 27 days of water curing and 2 days of air curing. Fig. 4.2 also illustrates the shrinkage after 6 days of water curing and 2 days of air curing and Fig. 4.2 illustrates the sealed shrinkage. Test 30, 31 and 32 is shrinkage after 6+2 days of curing and test 4, 8 and 12 is sealed shrinkage.
The LSC (31) and the VHSC (30) exhibit no significant change of shrinkage related to the curing. The HSC (32) exhibits an increased shrinkage when the curing period is reduced from 27 days of water curing to 6 days of water curing.

Apparently the shrinkage is to some extent discontinuous. Roughly, the shrinkage can be divided into two linear rates. The two rates cross approximately after 800-2000 hours of drying. The straight lines representing the two rates of shrinkage are illustrated in Fig. 4.2.

The shrinkage strains after 1 year of drying are illustrated in Fig. 4.3. Fig. 4.3 illustrates the shrinkage strains after 27+2 days of curing of sealed and unsealed specimens. The shrinkage strains are illustrated in relation to the compressive strength and the water/binder ratio.
Fig. 4.3 reveals that the shrinkage of unsealed specimens is decreased as the compressive strength is increased. The shrinkage of the VHSC is 40 % of the shrinkage of the VLSC with the same drying conditions.
The sealed specimens shrink less than the unsealed specimens. The reduced shrinkage due to

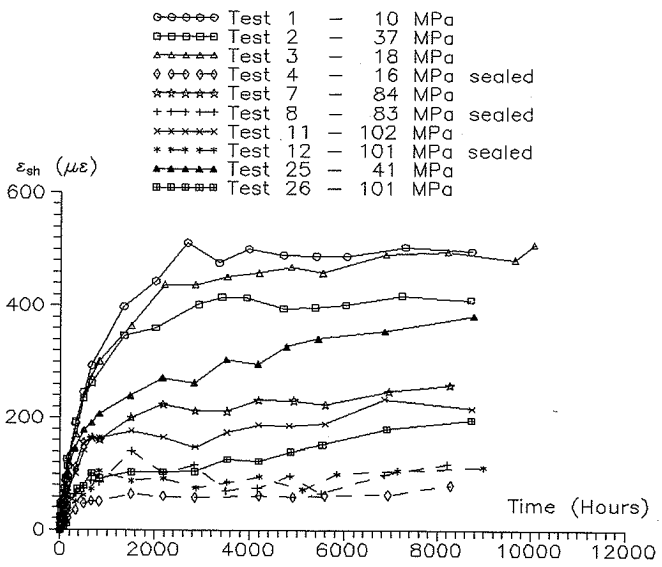

Fig. 4.1 The shrinkage of 7 concretes with compressive strength ranging from 10-100 MPa. Shrinkage of sealed concretes are presented too.

the sealing is valid for both LSC and VHSC. The shrinkage under sealed conditions is increased as the compressive strength is increased. The shrinkage of the LSC is 73 % of the shrinkage of the VHSC under sealed conditions. The shrinkage of the unsealed specimens exhibit a linear relation between the shrinkage and the compressive strength. Based upon the test results a linear relation between the shrinkage under sealed conditions and the compressive strength can be found too.

The ratio between the shrinkage of the unsealed LSC and the sealed LSC is 6.25. The same ratio for VHSC is reduced to 1.82

According to the non-linear relation between the compressive strength and the water/binder ratio a non-linear relation between the shrinkage and the water/binder ratio is a corollary. Based upon the linear relation between the shrinkage and the compressive strength and the non-linear relation between the compressive strength and the water/binder ratio, the relation between the water/binder ratio and the shrinkage can be determined. This has been done in Fig. 4.3 for the unsealed specimens and is illustrated by the solid line.

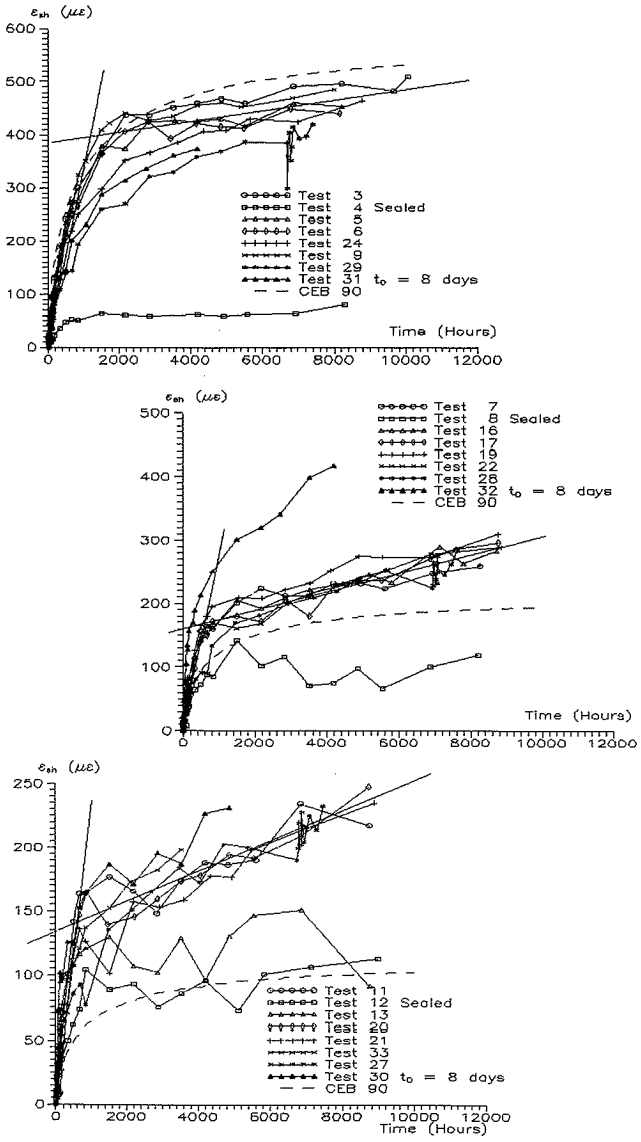

Fig. 4.2 Shrinkage of mix no. 2,5 and 6 (LSC, HSC and VHSC) under different curing and different environmental conditions. The straight lines illustrate the two rates of shrinkage. CEB for 65 % RH.

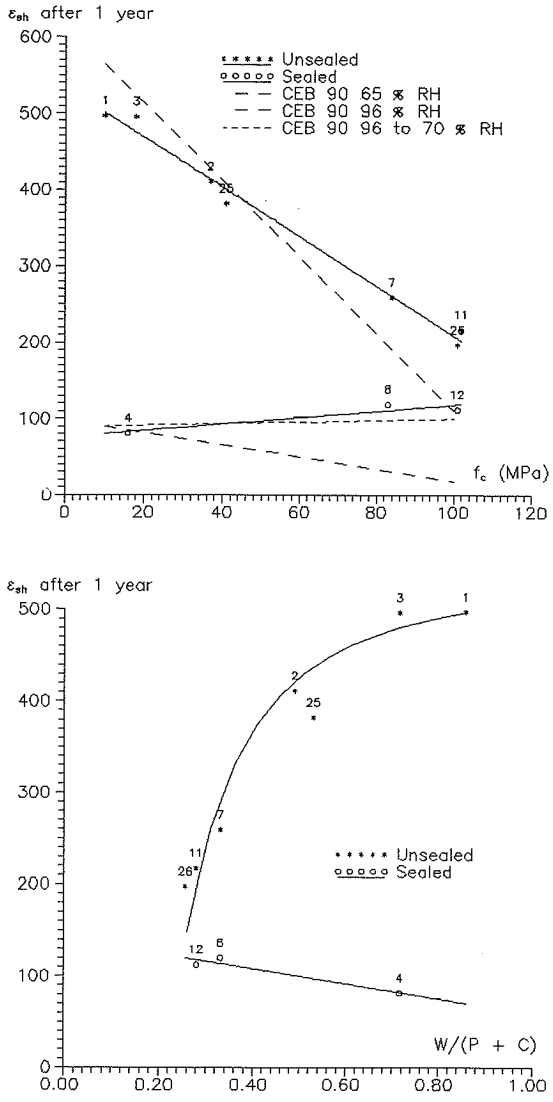

Fig. 4.3 The shrinkage after 1 year of 7 different concretes exposed to drying and 3 of the 7 concretes under a reduced drying.

Carbonation

In addition to the shrinkage tests, the depth of the carbonation has been determined after a period of approximately 1.5 years. In order to estimate the consequence of carbonation shrinkage the carbonation has been determined by means of a phenolphthalein solution. The carbonation test has been conducted approximately 1 month after unwrapping the sealed specimens as they were unloaded for thin-section analysis. The specimens have been split in the same way as for a split test.
The phenolphthalein test has revealed a penetration by CO_2 of 3.5 mm of the sealed specimens and 12.5 mm of the unsealed specimens of LSC. The HSC and the VHSC have not suffered any carbonation.

4.2 Discussion

Considering the shrinkage of the sealed specimens, it must be emphasized that the LSC (4) has an aggregate content of 84 % while the HSC (8) and the VHSC (12) have an aggregate content of 78 % which will cause a relative increase of the shrinkage of the HSC and the VHSC in relation to the LSC [56.1].

Mikkel Knudsen and Niels Gottlieb [91.6] have investigated the selfdesiccation of the very same concretes as investigated in this research. Mikkel Knudsen and Niels Gottlieb observed a reduction of the relative humidity to 78.5 % inside the VHSC 300 hours after the concrete has been cast. The relative humidity inside the HSC was reduced to 83.5 % after 500 hours. The LSC showed no significant selfdesiccation. The relative humidity inside the LSC was only reduced to 98 % after 500 hours.

The effectiveness of the sealing has been controlled by the weight-loss during the shrinkage period. The weight-loss of the sealed specimens indicate that the sealing has prevented 75 % of the weight-loss in relation to the weight-loss of the corresponding specimens exposed to drying over a period of 1 year. The relative reduction of evaporation of water is the same for the LSC, the HSC and the VHSC i.e. the 3 sealed concretes have lost 25 % water in relation to the unsealed concretes.
The unsealed LSC looses 25 % of the 1 year weight-loss after 3 days of drying, the unsealed HSC looses 25 % after 7 days while the VHSC looses the same percentage of water in 21 days.
Because of the insufficient sealing, the shrinkage of the sealed specimens will be referred to

as semi-basic shrinkage.

The three above mentioned subjects enhance each other and cause a larger shrinkage as the compressive strength is increased.

The tests of the pastes of the HSC (39) and the VHSC (38) have revealed the relation between concrete shrinkage ($\epsilon_{sh,concrete}$) and the shrinkage of the neat cement paste ($\epsilon_{sh,paste}$). The relation

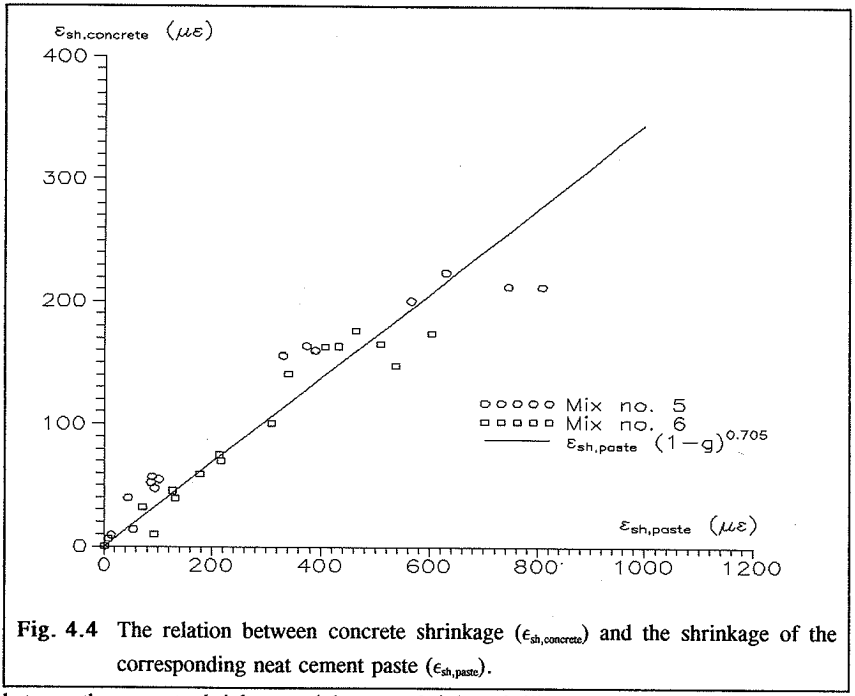

Fig. 4.4 The relation between concrete shrinkage ($\epsilon_{sh,concrete}$) and the shrinkage of the corresponding neat cement paste ($\epsilon_{sh,paste}$).

between the concrete shrinkage and the paste shrinkage is illustrated in Fig. 4.4. The exponent (n) of the equation for the VHSC in {4.1} is determined to 0.71 and to 0.70 for the HSC in relation to test number 7 and 11. Pickett [56.1] reported the exponent as 1.7 based upon test results on LSC and NSC. g is the aggregate content.

$$\varepsilon_{sh,concrete} = \varepsilon_{sh,paste} \cdot (1 - g)^{n} \qquad \{4.1\}$$

Using the exponent 0.70 and an aggregate content of 0.84 instead of 0.78 the LSC can be compared to the VHSC without the influence of the different aggregate content.

An increase of the aggregate content by 6 % will decrease the shrinkage of the HSC and the VHSC by 20 %.
Considering the reduction of shrinkage caused by an increased aggregate content the semi-basic shrinkage is indifferent as to whether the concrete is a LSC or a VHSC.

A number of tests [91.2] has proven that a decreased shrinkage in relation to an increased compressive strength for concretes exposed to drying.
While a decreased shrinkage during drying is well documented for higher compressive strength, it is more ambiguous as to whether there is any difference between sealed and unsealed shrinkage of concretes with high compressive strength.
Some tests [91.2] indicate no significant drying shrinkage of HSC, but confirm a significant drying shrinkage of LSC and NSC. On the other hand, a number of tests reveal a relation between the shrinkage of HSC and the ambient humidity.

The test results in this investigation reveal that there exists a difference between sealed and unsealed shrinkage, i.e. drying shrinkage $\neq 0$. The drying shrinkage of the VHSC is at least 55 % of the total shrinkage during drying.
Drying shrinkage is increased by carbonation. Carbonation is decreased as the strength is increased. The effect of carbonation enhances the shrinkage due to evaporation of water of the LSC, while the HSC and VHSC are unaffected by carbonation and therefor exhibit a decreased drying shrinkage.

4.3 Shrinkage and the CEB-FIP modelcode 1990

The shrinkage prediction method of CEB-FIP modelcode 1990 is a product formula. The factors of the formula depends on the compressive strength, the type of cement, relative humidity, age of the concrete and the time of drying. The two factors of concern in relation to this investigation are the strength factor and the time factor.

The relations between some of the test results and the CEB-FIP model are illustrated in Fig. 4.3. A poor correlation is observed for shrinkage at 65 % RH. The only parameter which is not rigorously determined is the type of cement in relation to the CEB definition of cement. The CEB-FIP model does not involve the use of microsilica fume or fly-ash.
Variation of the cement type factor does not reveal a better correlation, because the CEB-FIP model states that a concrete with a compressive strength of 90 MPa shrinks independently on the cement type. The shrinkage of a 90 MPa concrete is a fixed value in the model.

The CEB-FIP model is based upon a linear relation between the shrinkage and the concrete compressive strength and does not concern the relative humidity in relation to the compressive strength. The CEB-FIP model predicts a decrease of the shrinkage as the compressive strength is increased for sealed and unsealed specimens. A corollary of this texture of the model is a fixed ratio between drying shrinkage and basic shrinkage, which is in conflict with the mechanisms of reduced loss of water and no carbonation shrinkage in HSC.
The CEB-FIP model does not relate the relative humidity inside the concrete, due to selfdessiccation, and the compressive strength. A better relation between the CEB-FIP model and the test results can be achieved for the sealed specimens, assuming the relative humidity to be 70 % inside the VHSC as caused by selfdesiccation.

In Fig. 4.5 the time factor of the CEB-FIP model is illustrated. The dashed curves have been fitted to account for the poor correlation between shrinkage and compressive strength.

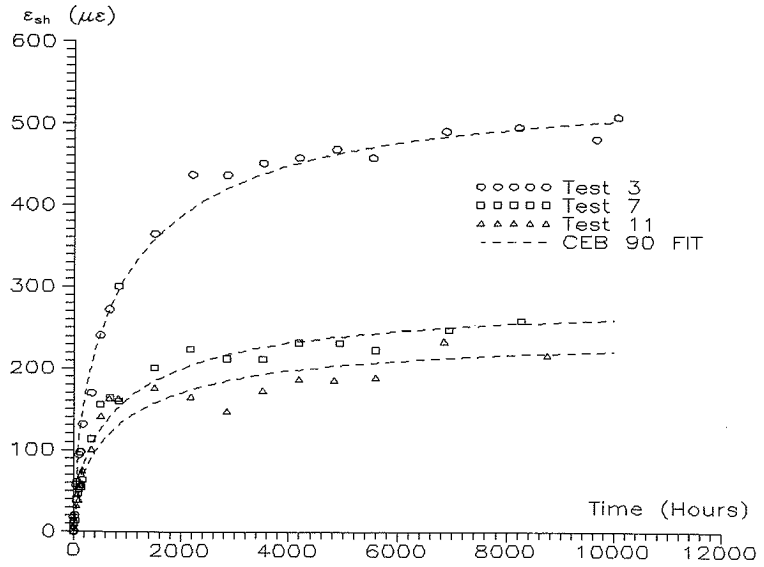

Fig. 4.5 The relation between the fitted time-function of the CEB-FIP modelcode 1990 and the test results.

The time function is a hyperbolic-power equation as in {4.2}.
$\epsilon_{sh,\infty}$ is the final shrinkage ($t \to \infty$), t is the time in days after casting the concrete, t_s the time in days of shrinkage start, k is a factor related to the specimen size. Equation {4.2} correlates

$$\varepsilon_{time} = \varepsilon_{sh,\infty} \cdot \left[\frac{t - t_s}{k + t - t_s} \right]^{0.5} \qquad \{4.2\}$$

quite well to the test results as demonstrated in Fig. 4.5.

Based upon the CEB-FIP time function a prediction of the final shrinkage reveals the values in Table 4.1. The values in Table 4.1 are based upon measurements for a period of 1 year and test results for a period of 1 month.

Table 4.1 *The final shrinkage ($\epsilon_{sh,\infty}$) based upon the CEB-FIP time function and test results for a period of 1 month and 1 year.*

Test number	1 month (A)	1 year (B)	B/A
3	511	554	1.08
7	300	286	0.95
11	295	244	0.83

4.4 Conclusions

1. Shrinkage of high-strength-concrete exposed to drying is reduced in direct proportion to the increase of compressive strength. The shrinkage of a high-strength-concrete exposed to drying is reduced due to the small amount of evaporable water, the dense structure of the paste and due to the lake of carbonation of high-strength-concrete.

2. The inadequate sealing allows no rigorous conclusions concerning the selfdesiccation or autogenous shrinkage. Despite of the inadequate sealing it can be concluded that a significant drying shrinkage of high-strength-concrete exists.

3. The relation between the shrinkage of neat cement paste and high-strength-concrete can be determined by the equation {4.1} using the exponent 0.7.

4. The CEB-FIP modelcode 1990 underestimate the 1 year shrinkage of the high-strength-concretes investigated by 100 %. It must be emphasized that the investigated concretes contain both plasticizer and pozzolans, which exceeds the range of application of the CEB-FIP model.
The time function of the CEB-FIP model is able to predict the relation between shrinkage and time quite well even for a small amount of test results.

5 CREEP OF CONCRETE

The concrete creep determined in the test report is in general analyzed in this section. The creep is analyzed in relation to the compressive strength and the aggregate content. The analysis of the aggregate content reveals an influence of load-induced microcracks. The test results are considered in relation to the CEB-FIP modelcode 1990, which is an emperical model calibrated to test results.

5.1 Experimental results

In Fig. 5.1 the creep strains of the 7 different concretes and the 3 sealed concretes are presented. The stress/strength ratios (σ/f_c) are 1/3. The creep strains illustrated in Fig. 5.1 are the creep strains of the specimens which have been loaded after 29 days of curing.
Fig. 5.1 shows that all creep curves follow the same trend/shape and do not cross one another in any significant way except of crossings related to test scatter or unless the environmental conditions are different. This observation allows an analysis based upon the 1 year creep.
Fig. 5.1 illustrates that the HSC (7,8) and the VHSC (11,12,26) exhibit the same creep strains independent on the compressive strength and the environment.
In Fig. 5.2 the creep strains of mix no. 2,5 and 6 (LSC, HSC and VHSC) are illustrated. The creep strains for stress/strength ratios ranging from 33 % to 70-75 % are illustrated in Fig. 5.2. The creep strains under sealed conditions and the creep strains at different loading ages are presented in Fig. 5.2 too. The test conditions are shown in the figure.
The LSC creeps less under sealed conditions than under unsealed conditions during the whole creep period. The creep of the HSC and the VHSC are indifferent as to whether the concrete is sealed or not. This is valid during the whole creep period.
The creep strains do not exhibit the same discontinuity as the shrinkage strains in section 4.

The LSC (31) loaded after 8 days exhibits creep strains less than the LSC (3,29) loaded after 29 days. The HSC (32) and the VHSC (30) loaded after 8 days exhibit creep strains larger than the HSC (7,28) and the VHSC (11,27) loaded after 29 days. At the time of loading the stress level is determined by the compressive strength at the time of loading. A concrete loaded after 8 days must be considered as a different concrete than the same concrete loaded after 29 days. Comparing the two "different" concretes loaded at different times requires an analysis based upon the specific creep or the creep coefficient. The influence of the age at loading is analyzed further in section 8. The influence of the stress/strength ratio is analyzed in section 9.

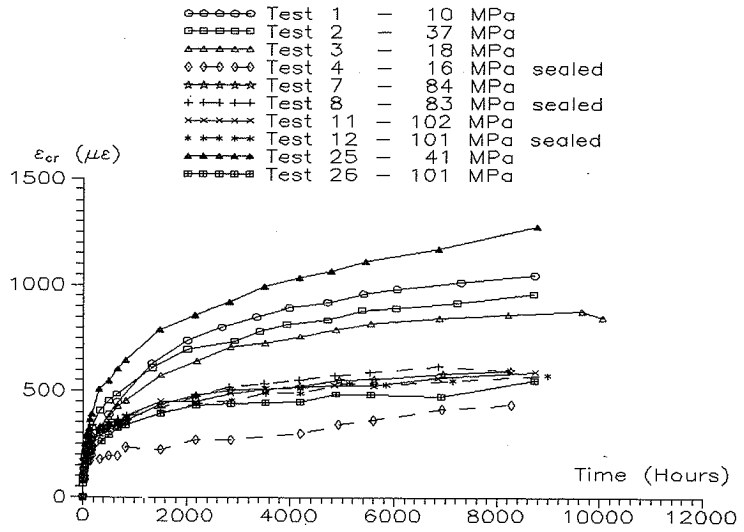

Fig. 5.1 The creep strains of 7 concretes with compressive strength ranging from 10 to 100 MPa. Creep strains of sealed concretes are presented too.

The creep coefficients after 1 year of creep are illustrated in Fig. 5.3. Fig. 5.3 represents the creep coefficients of sealed and unsealed specimens loaded to a stress/strength level of 1/3 and after 29 days of curing. The creep coefficients are illustrated in relation to the compressive strength and the water/binder ratio.

Fig. 5.3 reveals that the creep coefficients of unsealed specimens are decreased as the compressive strength is increased and the creep coefficients exhibit the same behavior during reduced drying. The creep coefficient of the VHSC is 12 % of the creep coefficient of the VLSC exposed to drying. During reduced drying the creep coefficient of the VHSC is 39 % of the creep coefficient of the LSC.

The creep coefficients are less during reduced drying. The reduction of the creep coefficients due to the reduced drying is not valid to the same extent for the HSC and the VHSC as for the VLSC. The HSC and the VHSC exhibit no drying creep.

The ratios between the creep coefficients of specimens exposed to drying in relation to the sealed specimens are 2.13 for the LSC and 1.05 for the VHSC.

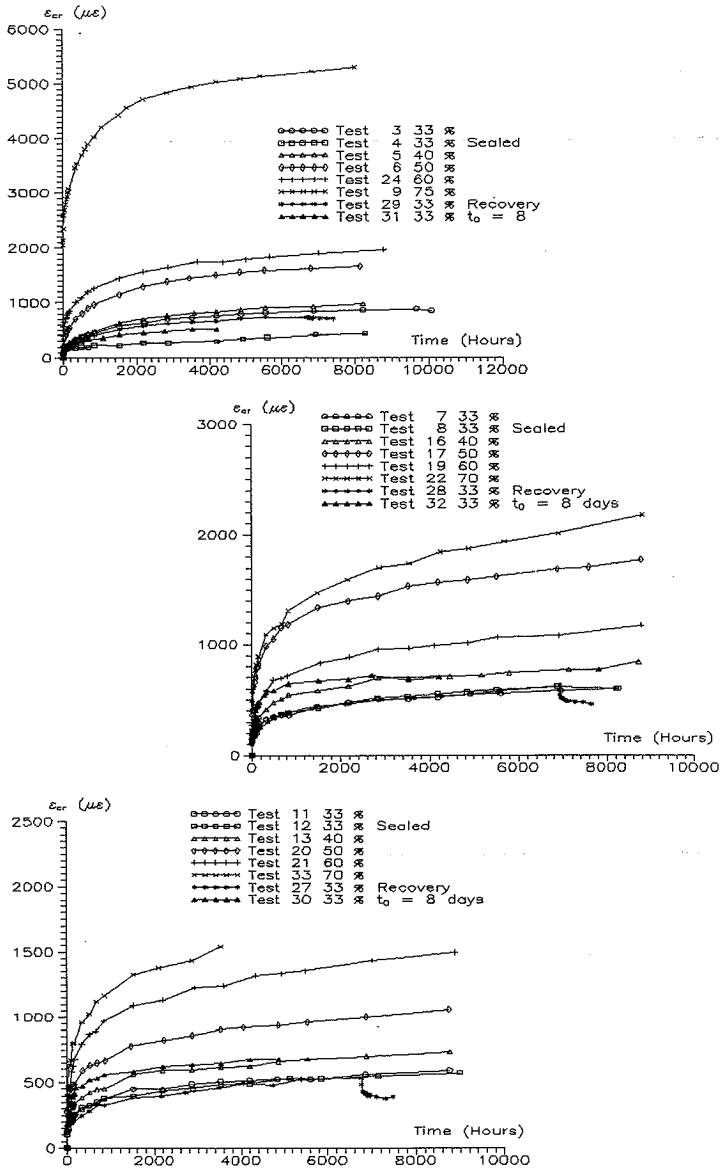

Fig. 5.2 Creep strains of mix no. 2,5 and 6 (LSC, HSC and VHSC) under different curing -, environmental - and stress/strength conditions.

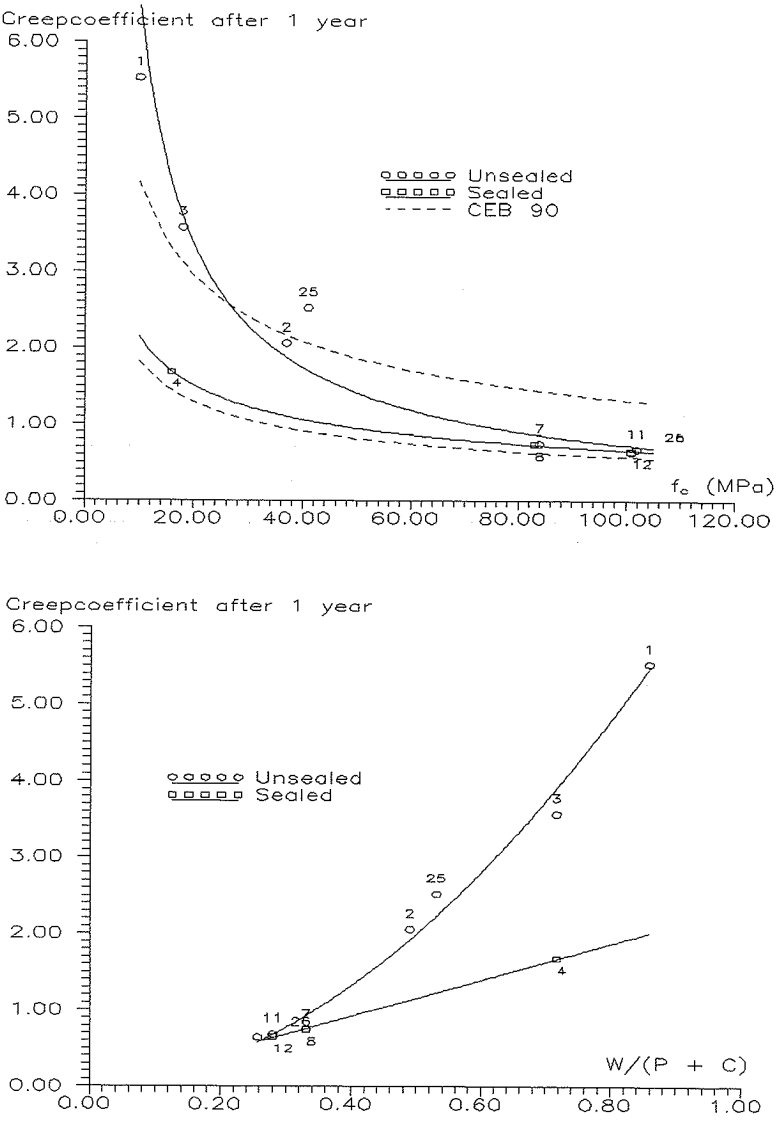

Fig. 5.3 The creep coefficients of 7 different concretes exposed to drying and 3 of the 7 concretes exposed to a reduced drying.

The relation between the compressive strength and the creep coefficients during drying and reduced drying is a power function as in {5.1}.

$$\varphi = a \cdot f_c^{\,b} \qquad \{5.1\}$$

The coefficients in {5.1} are presented in Table 5.1.
The non-linear power relation between the compressive strength and the water/binder ratio causes a new power relation between the creep coefficient and the water/binder ratio due to {5.1}.

Table 5.1 *Coefficients in the power function {5.1} related to the environmental conditions.*

Environment	a	b
Drying	57.8	-0.95
Reduced drying	6.89	-0.51

5.2 Discussion

The same factors which were discussed in the analysis of shrinkage must be considered in relation to creep too.
Because of the insufficient sealing the creep during reduced drying will be referred to as semi-basic creep.
The difference in aggregate content does not influence the relation between the creep coefficient and the compressive strength during drying and reduced drying in any confusing way. A modification of the aggregate content will increase the differences between concretes with low strength and concretes with high strength.

The tests of the pastes corresponding to the HSC (39) and the VHSC (38) reveal the relation between concrete creep strains ($\epsilon_{cr,concrete}$) and the creep strains of the neat cement paste ($\epsilon_{cr,paste}$). The relationship between concrete creep strains and creep strains of the pastes is illustrated in Fig. 5.4. In relation to test number 7 and 11 the components in equation {5.2} are determined.

$$\varepsilon_{cr,concrete} = \varepsilon_{cr,paste} \cdot (1 - g)^{m} + \varepsilon_{crack} \qquad \{5.2\}$$

In equation {5.2} g is the aggregate content.

The relation between the creep of the neat cement paste and the creep of the concrete reveals that ϵ_{crack} is not zero, as it was confirmed by the shrinkage analysis. The fact that $\epsilon_{crack} \neq 0$ indicate that strains in addition to the strains related to the composite analogy take place.

In section 1 it was pointed out that the differences in the mechanical properties of the neat cement paste and the aggregate might cause microcracks as a load is applied to the concrete specimens. The additional strains in {5.2} might be due to microcracks. It must be emphasized that the ϵ_{crack} values are in the order of magnitude of the accuracy of the measurements, and that a wrong determination of the initial strain as emphasized by Anders Nielsen [72.1] might cause some disturbance.

Anyway $\epsilon_{crack} \geq 0$ is a fact from two tests and a change of the initial strain will move the zero point which demands an explanation.

The exponent (m) is determined to be 1.10 for the HSC and to 1.18 for the VHSC. Neville [83.7] reported that the exponent tend to be 1 in relation to creep. Assuming ϵ_{crack} to be zero the exponent of the HSC becomes 0.99 and for the VHSC the exponent becomes 1.06.

Using the exponent 1.18 and replacing the aggregate content 0.84 by 0.78 and not considering ϵ_{crack} the LSC can be compared in relation to the VHSC without the influence of the different aggregate contents. An increase of the aggregate content by 6 % will decrease the creep of the VHSC and the HSC by 30-31 %.

Previous tests [91.2] confirm the decrease of the creep coefficient as the compressive strength is increased. A dominant part of the same tests confirms that drying creep of HSC does not exist.

Ali S. Ngab [80.1] even found a negative drying creep after 3 months. As pointed out in section 2, assuming the basic shrinkage to be zero may cause negative drying creep.

5.3 Creep and the CEB-FIP modelcode 1990

Like the shrinkage prediction method, the creep prediction method is a product formula. The factors of the model are dependent on age at loading, time of loading, the environmental conditions, the compressive strength, size of the specimen and the stress/strength ratio. In this section only the strength factor and the time factor will be considered.

In Fig. 5.3 the relations between the creep coefficients and the compressive strength according

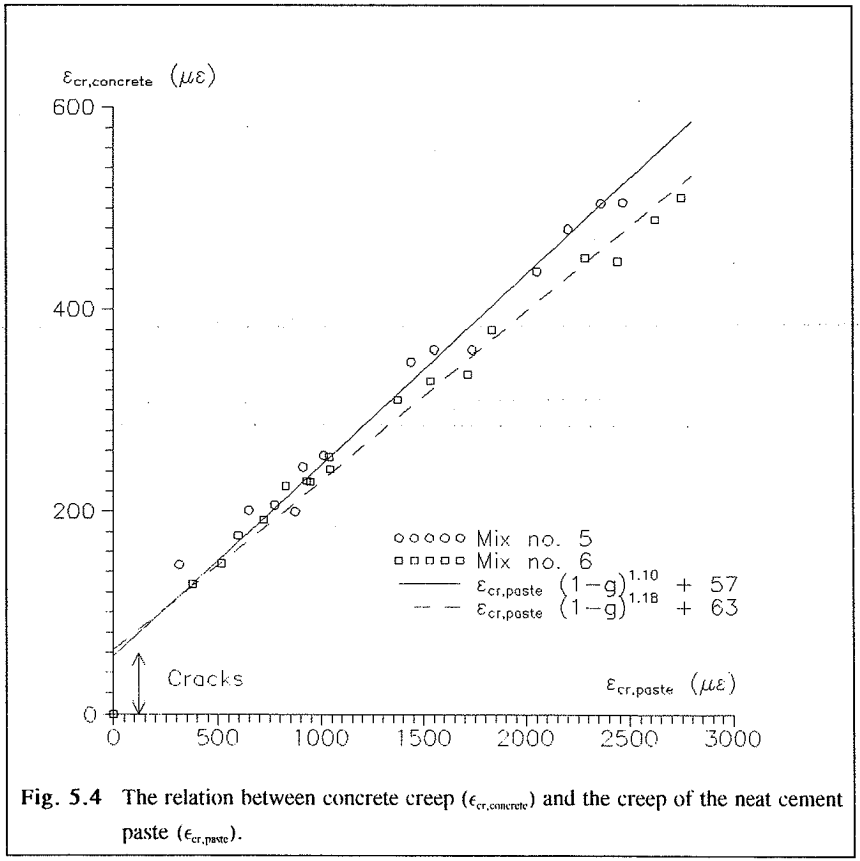

Fig. 5.4 The relation between concrete creep ($\epsilon_{cr,concrete}$) and the creep of the neat cement paste ($\epsilon_{cr,paste}$).

to the CEB-FIP approach are illustrated in relation to the test results.
Fig. 5.3 reveals a good correlation between the CEB-FIP approach for sealed specimens (RH assumed = 96 %). The correlation between the CEB-FIP model and the test results is poor as far as the unsealed specimens are concerned.

Basically, the product approach prescribes a constant ratio between the creep coefficient of the sealed specimens and the unsealed specimens. Using the product approach in relation to shrinkage, the same consequence is observed.
The basic product approach considers the involved factors as independent on one another. This is, according to the mechanism of shrinkage and creep, not true.
The porosity of the concrete and the compressive strength are related. Increased porosity ⇒

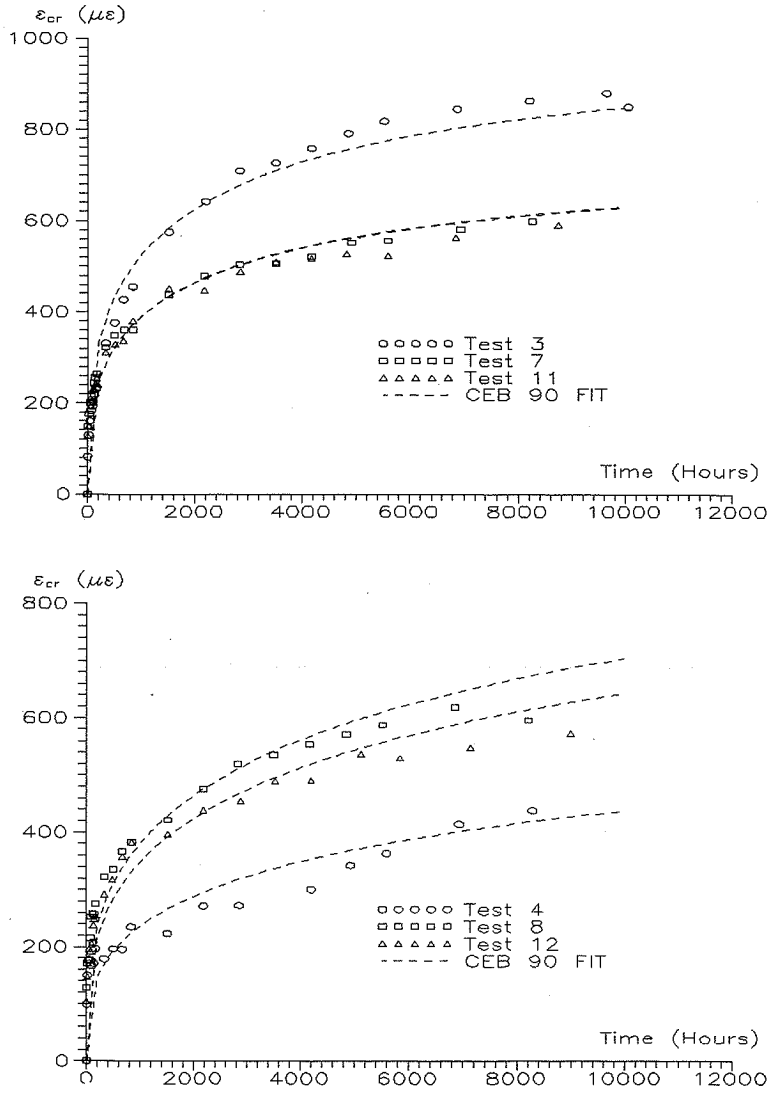

Fig. 5.5 The relation between the fitted time-function of the CEB-FIP modelcode 1990 and some test results.

decreased compressive strength and visa versa. As the compressive strength is increased the concrete becomes more dense and the diffusion related to the environmental conditions is decreased. A corollary is that a constant ratio between drying creep and basic creep cannot exist, as the test results confirm.

The CEB-FIP model proposes {5.3} as the relation between the compressive strength and the creep coefficient. {5.3} is independent on the relative humidity.

$$\varphi = \frac{A}{\sqrt{f_c}} \qquad \{5.3\}$$

The exponents in Table 5.1 can be compared to {5.3}.

The CEB-FIP time function for creep is as for shrinkage a hyperbolic-power equation as presented in {5.4}.

$$\varepsilon_{time} = \varepsilon_{cr,\infty} \cdot \left[\frac{t - t_0}{m + t - t_0}\right]^{0.3} \qquad \{5.4\}$$

$\epsilon_{cr,\infty}$ is the final creep, t is the time in days after casting the concrete, t_0 is the time in days at loading, m is a factor related to the ambient humidity and the specimen size. In Fig. 5.5 the relations between the time function and some test results are illustrated. The time function has been fitted to account for the poor correlation between strength and creep.
Fig. 5.5 reveals a good correlation between the test results and the time function.

Table 5.2 *The final creep ($\epsilon_{cr,\infty}$) based upon the CEB-FIP time-function and test results over a period of 1 month and 1 year.*

Test number	1 year (A)	1 month (B)	B/A
3	1009	851	0.84
4	667	810	1.21
7	750	811	1.08
8	1074	1241	1.16
11	748	821	1.10
12	981	1170	1.19

Based upon the CEB-FIP time-function, predictions of the final creep gives the values in Table 5.2.
Table 5.2 reveals that the CEB-FIP creep time-function needs more test results to predict the final creep than the CEB-FIP shrinkage time-function.

5.4 Conclusions

1. Creep of high-strength-concrete exposed to drying is reduced exponentially in relation to an increase of the compressive strength. The creep of high-strength-concrete exposed to drying is reduced due to the small amount of evaporable water in the concrete and the dense structure of the paste.

2. Keeping the inadequate sealing in mind, high-strength-concrete apparently exhibits no drying creep.

3. The relation between the creep of neat cement paste and high-strength-concrete can be determined by {5.2} using the exponent 1.14 as an average.

4. Microcracks are indirectly identified, and caused by the divergence between the composite components.

5. Keeping the mix proportions in mind, the CEB-FIP modelcode 1990 overestimates the creep coefficient of high-strength-concrete by 90 %.
   The fitted time-function of the CEB-FIP approach is able to predict the relation between creep and time quite well, but not for a small number of test results.

6 WEIGHT-LOSS

This section concerns the measured amount of evaporated water from the concrete specimens. The relation between the shrinkage and the evaporated amount of water is discussed. The relation between creep and shrinkage specimens are analyzed in relation to the weight-loss.

6.1 Experimental results

In Fig. 6.1 the weight-loss during the time of drying is presented. The weight-loss in Fig. 6.1 is the weight-loss of unloaded shrinkage specimens.
The LSC (3) exposed to drying after 27 days of water curing exhibits the largest weight-loss. The weight-loss is decreased as the compressive strength is increased. The weight-loss of the pastes exhibits the same behavior and is larger than the weight-loss of the corresponding concretes.
The weight-loss of the concretes exposed to drying after 6 days of water curing also decreases as the compressive strength is increased.
The weight-loss of the LSC (31) exposed to drying after 6 days is less than the weight-loss of the LSC (3) exposed to drying after 27 days. The HSC (7,32) exhibits the opposite behavior while the VHSC is more or less indifferent as to whether the concrete is exposed to drying after 6 days or 27 days of water curing.
The weight-loss of the LSC (3,31) becomes constant within one year of drying at 65 % RH. The HSC and the VHSC still loose water after one year.

The weight-loss of the loaded creep specimens has been determined for some test series after removing the load. The weight-loss of the creep specimens do not differ significant from the weight-loss of the unloaded shrinkage specimens.

6.2 Discussion

Fig. 6.1 reveals that the LSC contains more evaporable water than the HSC and VHSC. The increased amount of evaporable water is due to the higher water/cement ratio and subsequent higher porosity.
Hydration of the cement causes a chemical shrinkage which causes an increase of the porosity of the concrete. As the degree of the hydration increases, the amount of pores increases too. Curing concrete specimens in water during hydration allows water continuously to fill the

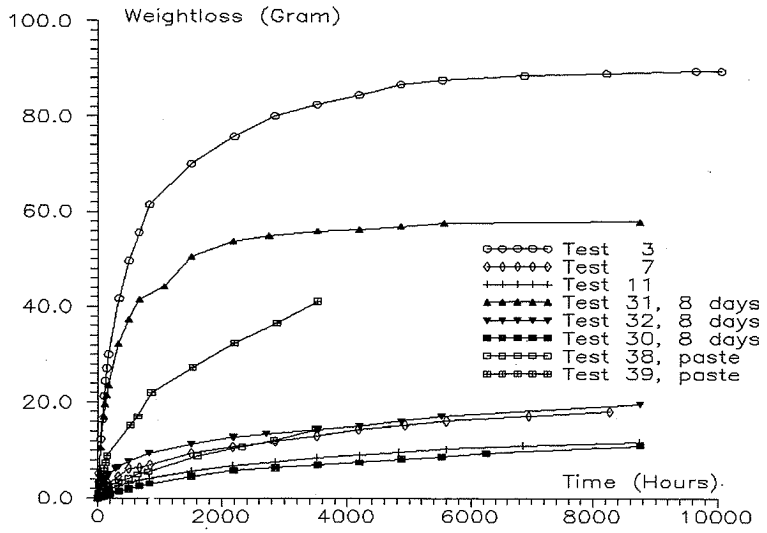

Fig. 6.1 Weight-loss after 6 days and 27 days of water-curing. The specimens have not been loaded.

voids caused by hydration as they develop. The filling of the pore-system is only possible if the pore-system is continuous.

The longer the concrete stays in water the more water it will adsorb, which is due to the time of diffusion and the increased amount of pores.

This mechanism reveals that the LSC cured in water for 6 days has not adsorbed as much water as the LSC cured 27 days in water.

In section 4 the shrinkage related to the weight-loss considered in this section reveals that the shrinkage of the LSC (31) cured 6 days in water is less than the shrinkage of the LSC (3) cured 27 days in water.

The HSC (7) exhibit larger shrinkage after 27 days of water curing than the HSC (32) cured 6 days in water.

The shrinkage of the VHSC (11) exposed to drying after 27 days is insignificantly less than the shrinkage of the VHSC (30) exposed to drying after 6 days.

Based upon this behavior it must be concluded that the shrinkage due to drying is related to the amount of the evaporable water to some extent.

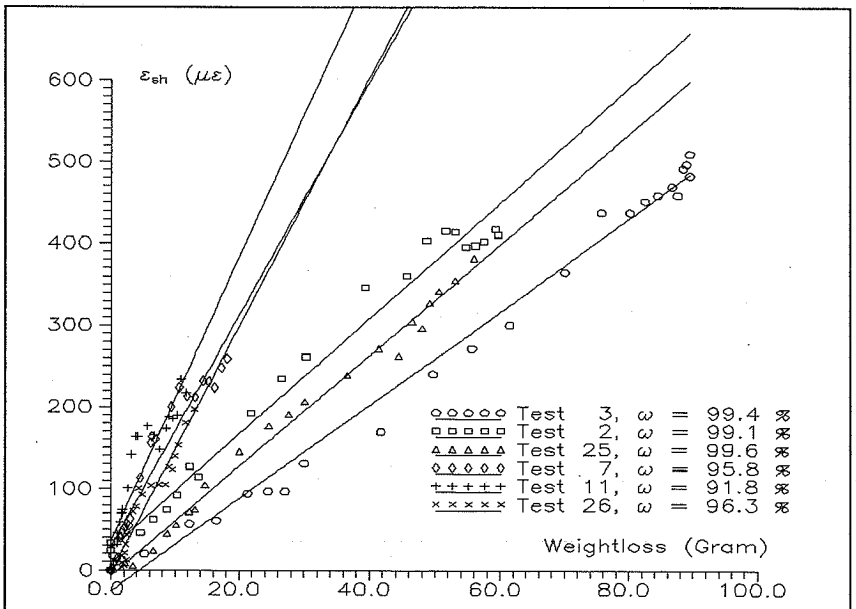

Fig. 6.2 Shrinkage in proportion to the weightloss. ω is the coefficient of correlation.

T.C.Powers [59.3] found a linear relation between the lost water and the observed shrinkage of cement-pulverized silica pastes.

In Fig. 6.2 the shrinkage is illustrated in relation to the corresponding weight-loss. The LSC and the NSC exhibit a linear relation between the shrinkage and the weight-loss. The correlation between a linear description between the shrinkage and the weight-loss of the HSC and the VHSC is fair. The decreased correlation between shrinkage and weight-loss of the HSC and the VHSC is probably due to selfdesiccation, which acts like drying but does not cause a weight-loss.

The dense structure of the HSC and the VHSC decreases the rate of diffusion, which means that they continue to evaporate water longer than the LSC.

It must be emphasized that carbonation of the concrete increases the weight. Carbonation is dependent on the moisture content in the concrete. The less moisture the larger carbonation. It has been determined that the LSC carbonates, which might cause a premature stabilization of the weight-loss due to evaporation of water. Evaporation might still take place.

Maney [41.1], Mamillan [59.2] and Neville [59.1] did not in their investigations find any different weight-loss of loaded specimens in relation to unloaded specimens. This does not

support the seepage theory unless evaporable water does not affect creep, or the accuracy of the measurement can not account for the effect.
V.Penttala & T.Rautanen [90.4] found that the loaded specimens lost less water than the unloaded specimens and concluded that the compaction of the pores due to the load increases the time of diffusion.
Penttala & Rautanen also found a good correlation between the evaporated amount of water and the shrinkage.

F. de Larrard & J-L.Bostvironnois [91.1] reveal by means of gammadensimetry that HSC and VHSC only dries out at the surface of the specimen while the core still remains in the original state of moisture content for several years.

6.3 Conclusions

1. Shrinkage of concrete exposed to drying is linearly correlated to the amount of evaporated water. Selfdesiccation shrinkage of HSC and VHSC disturbs the linear behavior of the proportionality between the shrinkage and the corresponding weight-loss.

2. HSC and VHSC do not contain as much evaporable water as LSC and as a corollary shrink less.

3. One unit of evaporated water causes more shrinkage in HSC than in LSC.

7 DEVELOPMENT OF STIFFNESS AND STRENGTH

The development of mechanical properties due to continued hydration is discussed in this section. The influence of high stress/strength ratios and development of microcracks are discussed. The influence of the development of the mechanical properties is evaluated in relation to static-fatigue.
The test results are evaluated in relation to the proposal of the CEB-FIP modelcode 1990. The strength loss of the pastes are also discussed.

7.1 Experimental results

In Fig. 7.1 the strength development of mix no. 2,5 and 6 (LSC, HSC and VHSC) are illustrated. The strength development of the neat cement paste of mix no. 5 and 6 are presented in Fig. 7.1 too. The strength development has taken place after 27 days of water-curing and 2 days of air-curing. During the strength development the specimens are cured in air.

In the period of time investigated, the concretes increase in strength. The neat cement pastes decrease in strength during the same period of air-curing. The strength loss is most significant for the VHS paste. The strength loss is due to severe cracks caused by restrained drying shrinkage. The cracks are visible to the naked eye and are of the type I and II shown in section 1.

In Fig. 7.2 and Fig. 7.3 the development of the strain corresponding to the stress applied to the creep specimens is illustrated. Fig. 7.2 and Fig. 7.3 illustrate the development of the initial strain in relation to the applied stress. The strain is denoted: "The true initial strain" (ϵ_o), see section 2.

The true initial strains of the concretes are decreased with time. The true initial strain of the pastes are increased because of the cracks.
As the true initial strain decreases, the elastic modulus increases at the same stress level.

The higher the stress at the time of loading the more significant is the influence of the development of stiffness. The influence of the high stress is more pronounced for the LSC and is decreasing as the strength is increased.

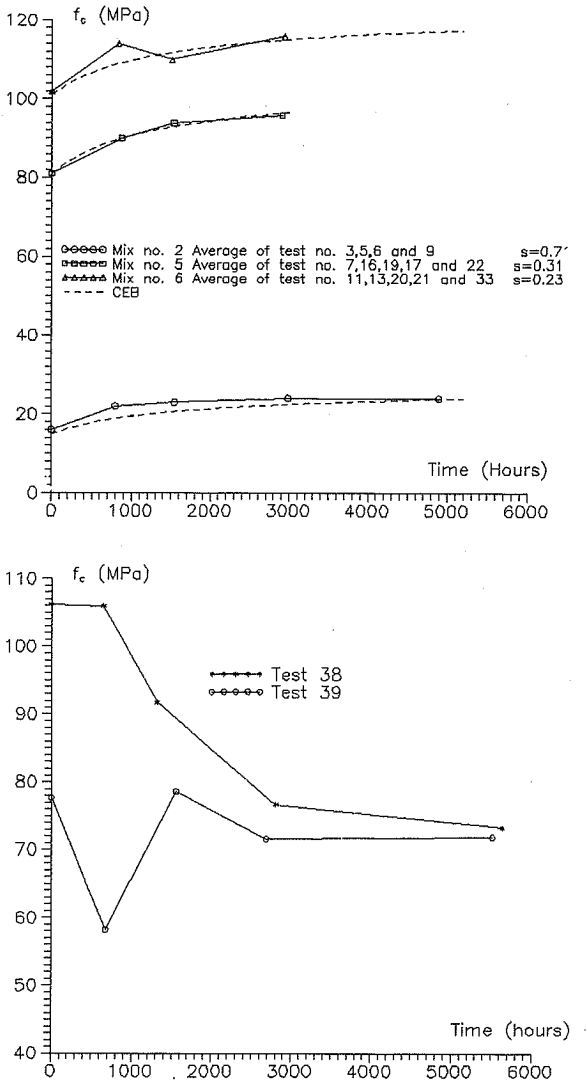

Fig. 7.1 Strength development of air cured LSC (2), HSC (5) and VHSC (6). Strength development of HS (39) and VHS (38) pastes. CEB modified.

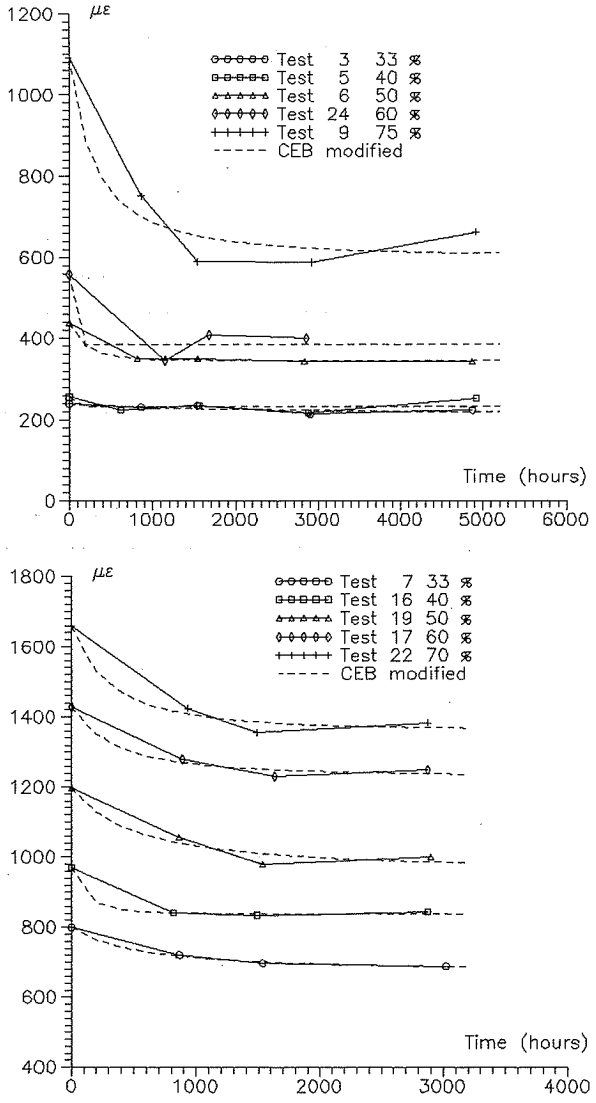

Fig. 7.2 Development of true elastic strain for respectively LSC and HSC.

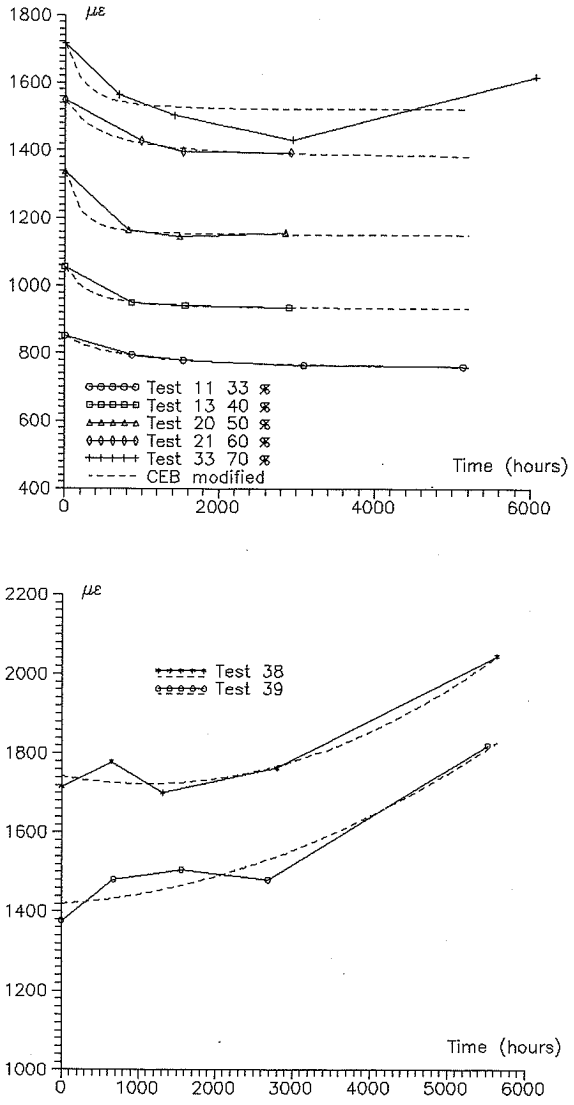

Fig. 7.3 Development of true initial strain of respectively VHSC and of HS (39) and VHS (38) pastes.

7.2 Discussion

The development of strength and elastic modulus are known to be dependent on the curing. Gilkey [26.1] proved in 1926 that the strength of a dry concrete is higher than the strength of a wet concrete. It was proven that a water curing interrupted after 4 weeks followed by air curing increased the rate of the compressive strength development in relation to the continuously water cured specimens. In 1951 W.H. Price [51.1] supported this conclusion, but proved that a decrease of the strength of the air cured specimens occured after a period of 90 days, while the water cured specimens still gained strength and actually surpassed the strength of the air cured specimens after approximately 120 days. The latter investigation involved concretes with water/cement ratios of 0.5.

Concretes containing silica-fume and HSC and VHSC containing silica-fume exhibit the same behavior according to Larrard and Bostvironnois [91.1], who considered the behavior as specific for high-strength-concrete containing silica-fume.

Silica-fume concretes cured in water did lose flexural strength according to Carette et al., [89.9] but this is not comparable to the mechanism involved in relation to the development of compressive strength. The flexural strength is very sensitive to cracks and silica-fume concretes often develop more microcracks which affects the flexural strength, while the compressive strength is not affected at the same rate.

The strength development is evaluated by means of the CEB-FIB modelcode 1990s strength development approach {7.1}

$$f_c(t) = f_{c,28} \cdot \beta(t) = f_{c,28} \cdot \exp\left[s \cdot \left(1 - \left(\frac{672}{672 + t} \right)^{0.5} \right) \right] \qquad \{7.1\}$$

The CEB-FIP approach proposes the s values in {7.2}

$$s = \begin{cases} 0.20 \text{ for rapid hardening cement} \\ 0.25 \text{ for normal hardening cement} \\ 0.38 \text{ for slowly hardening cement} \end{cases} \qquad \{7.2\}$$

$f_c(t)$ is the compressive strength at the time t in hours and $f_{c,28}$ is the compressive strength after 28 days. In Fig. 7.1 the s values have been determined by the least square method in relation to the test results and {7.1}.

The VHSC containing silica-fume develops the strength at a lower rate than the HSC containing silica-fume and fly-ash. The LSC containing fly-ash develops strength after the water curing period at a higher rate than the stronger concretes. This can be determined by means of the **s** values. The rate of the strength development is not just related to the type of

cement but also to the water/cement ratio. The development of the true initial strain in Fig. 7.2 and Fig. 7.3 are related to the development of the elastic modulus. In section 3 a relation between the compressive strength and the elastic modulus was discussed. The proposed relation between strength and modulus can not be used to predict the development of the elastic modulus in relation to the development of strength, as the modulus increase faster than the strength. A mathematical empirical relation between the development of the modulus and the strength is suggested. The relation is based on the CEB-FIP approach, but some of the parameters are determined in relation to the test results and does not have any physical relevance related to the number of minima which satisfy the least square method.

The non-linearity of the stress-strain relation of the concrete is related to the stress/strength ratio. As the strength increases the stress/strength ratio decreases and affects the secant modulus.
Based upon the CEB-FIP approach of strength development {7.1} and the development of the elastic modulus {7.3} the development of the true initial strain can be estimated as in {7.4}.

$$E_c = E_{c,28} \cdot \beta(t)^{0.5} \qquad \{7.3\}$$

$$\varepsilon_i(t) = \alpha \cdot \frac{1}{E_{c,28} \cdot \beta(t)^{0.5}} \qquad \{7.4\}$$

α is the stress/strength ratio at the time of applying the load to the creep specimens. CEB-FIP proposes 0.85 as the ratio between the initial modulus and the secant modulus. The ratio 0.85 corresponds to a stress/strength ratio corresponding to the secant modulus and as the stress/strength ratio is altered because of the strength development, the ratio 0.85 increase to 1.0 i.e. α might be considered as time-dependent too. To avoid further empirical complexity related to α and time, the exponents 0.5 in {7.1} and {7.4} have been changed and determined in relation to the test results. The exponents vary graetly and therefor have no physical meaning, but a reasonable mathematical relation between the development of the true initial strain and time can be stated. The mathematical relation illustrated by the dashed lines in Fig. 7.2 and Fig. 7.3 represents a CEB-FIP modified curve-fit. The dashed lines in Fig. 7.3 illustrating the development of the true initial strain of the pastes are not fitted to the CEB-FIP approach.

The development of strength, the stress/strength ratio and the limit of unstable crack-growth significantly affect the decrease of true initial strain at high stress/strength ratios.
The LSC (9) exhibits a large initial strain at the time of applying the sustained load at

stress/strength ratio of 75 %. After a period of time the strength has increased and the stress/strength ratio has decreased to 51 %. At this stress level no unstable crack-growth takes place.

The influence of the strength development and the related crack-limit affect creep and the static fatigue strength. The interplay between the shrinkage and the stress developing new cracks is reduced, and the reduction is enhanced by the increase of the tensile strength. This mechanism will reduce creep related to microcracks.

The influence on the static fatigue strength is quite similar. As an unstable crack is in progress related to the high stress/strength ratio, the influence of the increase of strength may cause a stabilization of the crack, and failure will not occur.

The significant decrease of the true initial strain at high stress of LSC indicates that the influence of strength development is more significant for LSC than HSC in relation to static fatigue.

Visible cracks can be observed at the surface of the concrete creep specimens in test 9. The stress-strain curve shows an increasing strain rate. The increased strain rate and the visible cracks indicate that the rate of the volume change is increased due to the cracking [91.3].

It is generally believed that an increased rate of volume change reveals the limit of static fatigue. The development of strength has overtaken the development of cracks and has stopped a static fatigue failure in progress.

7.3 Conclusions

1. The strength development rate after 27 days of water curing is confirmed to be slower for high-strength concrete than for low strength concrete.

2. The development of true initial strain is dependent on the stress/strength ratio and this effect is most significant for LSC.

3. The static fatigue strength is not only related to the stress/strength ratio, but also to the development of mechanical properties.

4. The development of mechanical properties is affected by cracks and is most significant in neat cement paste of high-strength.

8 AGE AT LOADING

*The age at loading after casting the concrete is analyzed in this section. The **Dischinger** approach and the CEB-FIP modelcode 1990 proposal are considered in relation to the test results.*

8.1 Experimental results

The LSC (3,31), the HSC (7,32) and the VHSC (11,30) have been loaded after 8 days and 29 days. In Fig. 8.1 the specific creep strains related to the loading age are depicted in relation to the time under load.
For LSC, HSC and VHSC the specific creep is decreased when the age at application of load is increased.
Approximately one year after applying the load, the specific creep of the LSC loaded after 29 days is 76 % of the specific creep of the LSC loaded after 8 days. The same ratio is 51 % for the HSC and 59 % for the VHSC.

8.2 Discussion

In 1930 Glanville [30.1] concluded from experimental results that the creep rate is independent on the age at loading. This hypothesis was treated further mathematically by Whitney [32.1] in 1932 and by Dischinger [37.1] in 1937.
The consequence of this rate of creep method (known as the "Dischinger approach") is that just one specific creep curve is needed to predict creep in relation to the age at application of load. The Dischinger approach is illustrated in Fig. 8.1.a in relation to the investigated concretes. Fig. 8.1.a reveals that the Dischinger approach underestimates the specific creep for LSC, HSC and VHSC. England & Illston [65.1] pointed out the underestimation of the creep and proposed the rate of flow method.
The CEB-FIP modelcode 1990 proposes a factor related to the age at loading. The factor is only dependent on the loading age i.e. the ratio between the LSC loaded after 29 days in relation to the LSC loaded after 8 days is the same for HSC and VHSC. The proposed ratio according to the CEB-FIP approach is 78 %, which corresponds well to the LSC but not to the HSC and the VHSC.

In Fig. 8.1.b the estimated specific creep of the concrete loaded after 8 days is shown as

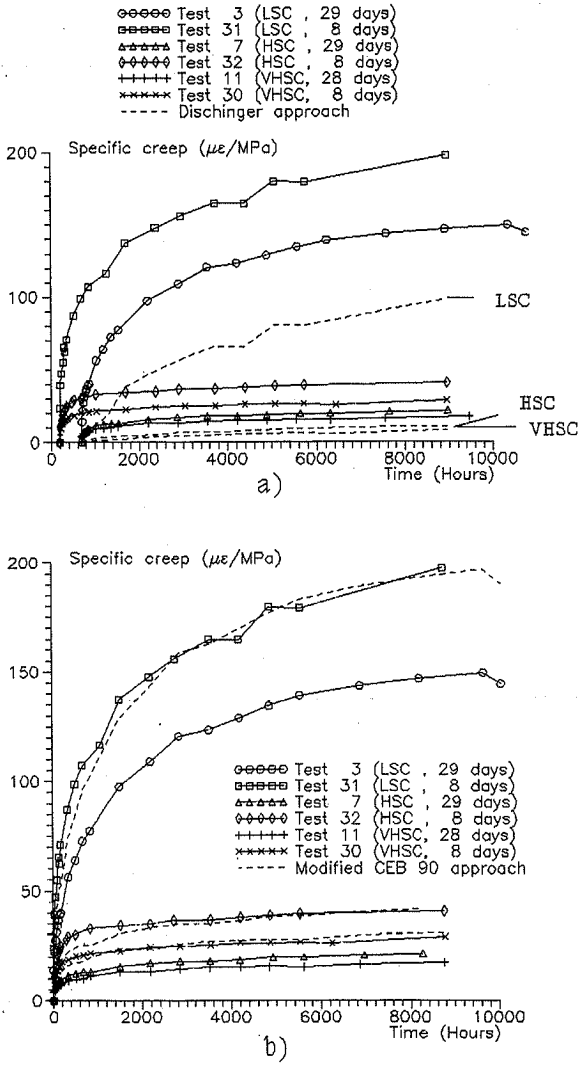

Fig. 8.1 Specific creep of LSC, HSC and VHSC loaded after 8 days and 29 days.

dashed curves. The dashed curves are determined on the basis of the specific creep of the concretes loaded after 29 days multiplied with a constant according to the CEB-FIP approach.

The age at application of load is related to the development of strength. When the development of strength has ceased the age at loading has no further significant influence on the creep.

8.3 Conclusions

1. The HSC and the VHSC exhibit the same behavior as the LSC as far as the age at application of load is concerned. The specific creep is decreased the older the concrete is at application of load.

2. The Dischinger approach is known to underestimate creep which has been confirmed for the LSC, the HSC and the VHSC.

3. The CEB-FIP approach predicts the relation between the specific creep of the LSC loaded after 8 days and 29 days quite well. The CEB-FIP approach do not predict the same ratio very well for the HSC and the VHSC.

9 THE STRESS/STRENGTH RATIO

The limit of linearity of creep is discussed in this section in relation to the test results. The influence of shrinkage-induced cracks during loading on the limit of linearity is analyzed. The stress/strength ratio is evaluated in relation to the CEB-FIP modelcode 1990 proposal.

9.1 Experimental results

In Fig. 9.1 the strains in relation to different stress/strength ratios are illustrated. The strains determined just after applying the load and the strains without shrinkage after ½-1 year are illustrated.
Linear regression lines are drawn. The regression lines of the LSC are based upon test results for $\sigma/f_c \leq 40$ %.
A linear relation between the stress/strength ratio and strains of the LSC can be observed for $\sigma/f_c \leq 40$ % of both short-time and long-time strains. At $\sigma/f_c = 60$ % a significant change in the proportionality between short-time strains and long-time strains take place.
The linear regression lines related to the short-time strains of both the HSC and the VHSC pass through the origin while the regression lines related to the long-time strains do not pass through the origin.

In Fig. 9.2, Fig. 9.3 and Fig. 9.4 the specific creep, and the creep coefficient of the LSC, the HCS and the VHSC are presented.

The specific creep reveals the relation between creep and the stress/strength ratio. A linear relation between creep and the stress/strength ratio causes specific creep relations which are independent on the stress/strength ratio.
The specific creep of the LSC illustrated in Fig. 9.2 shows that the creep is not linear at stresses exceeding 33 %.
The specific creep of the HSC in Fig. 9.3 indicate linearity between creep and the stress to a stress/strength ratio of 33-40 %.
The specific creep of the VHSC in Fig. 9.4 shows a linear relation between creep and stress to a stress/strength ratio of at least 40 % but not exceeding 50 %.

While the specific creep reveals the relation between creep and the stress/strength ratio , the creep coefficient reveals the relation between creep and the initial strain. As far as the stress/initial strain relation is linear, the creep coefficient reveals a linear relation between

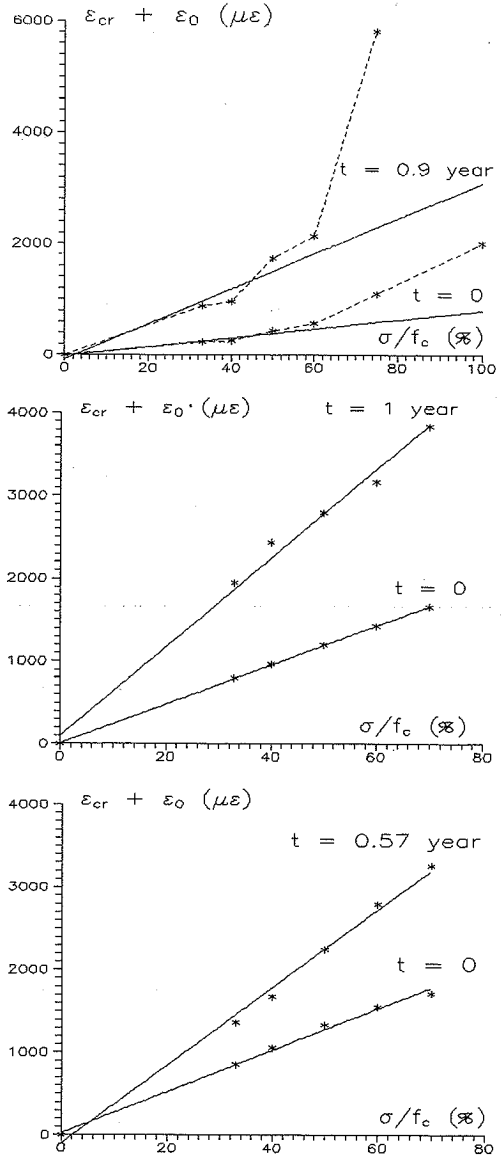

Fig. 9.1 Initial strain and total creep strain (no shrinkage strains) in relation to the stress/strength ratio of respectively the LSC, the HSC and the VHSC.

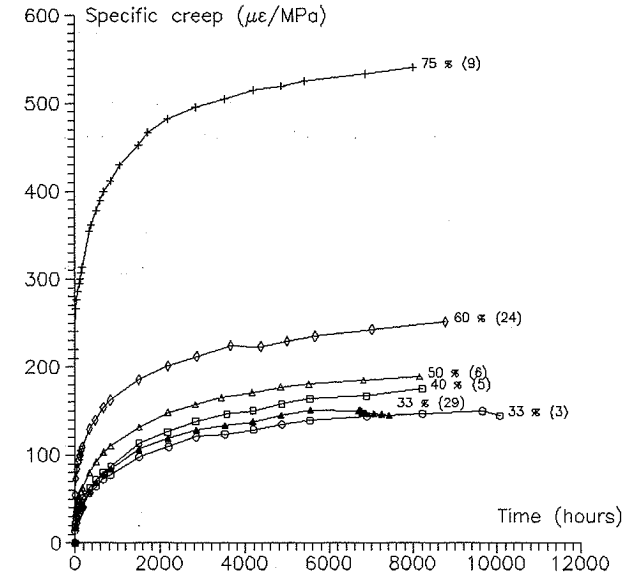

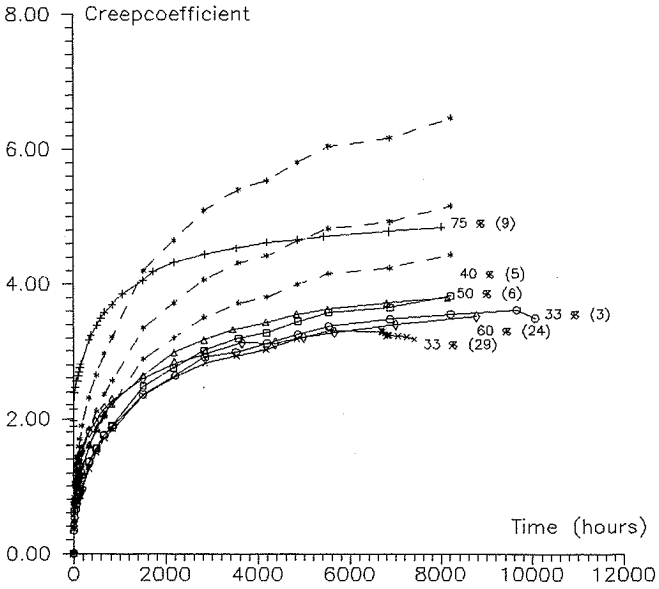

Fig. 9.2 Specific creep and creep coefficient of the LSC (mix no. 2). σ/f_c in %.

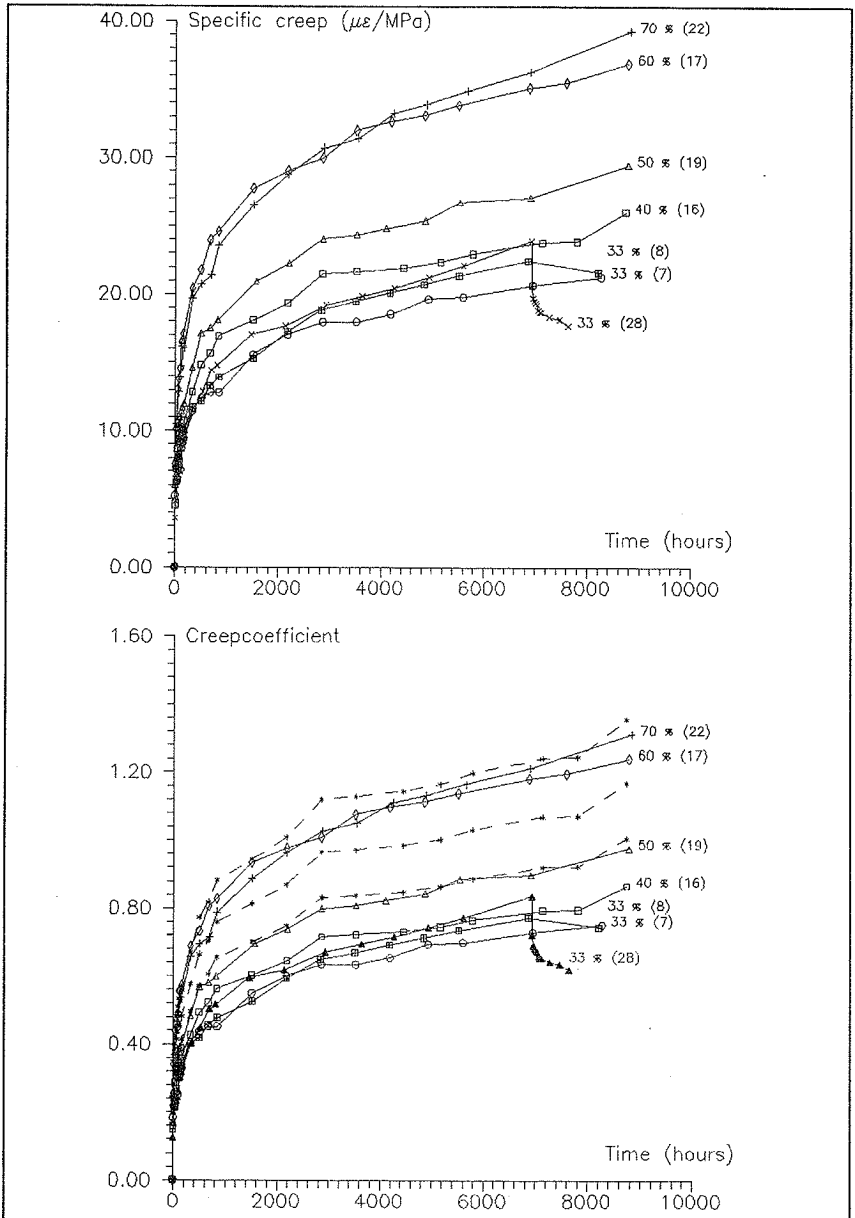

Fig. 9.3 Specific creep and the creep coefficient of the HSC (mix no. 5). σ/f_c in %.

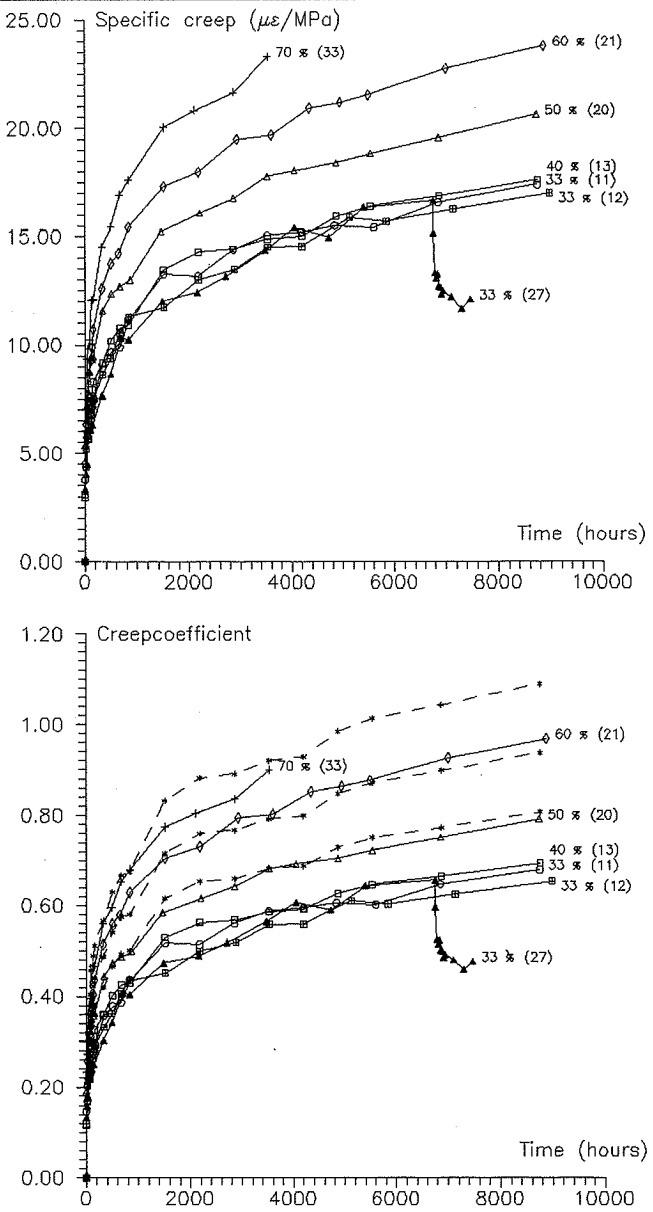

Fig. 9.4 Specific creep and creep coefficient of the VHSC (mix no. 6). σ/f_c in %.

creep and stress. If the stress/initial strain relation is not linear the creep coefficient can not be used to prove linearity between stress and strain, but can prove a linear relation between initial strain and creep.

Before an analysis of the creep coefficient is commenced, it must be emphasized as Anders Nielsen pointed out, that small values of creep coefficients are more sensitive to the determination of the initial strain.

The stress/initial strain relationship of the LSC in Fig. 9.1 is not linear at stresses exceeding 40 % of the strength. The creep coefficient in Fig. 9.2 shows a linear relation between the initial strain and the creep strain. This linear relation is valid for stresses less than 60 % of the strength.

The creep coefficients in Fig. 9.3 and Fig. 9.4 reveal a linear relation between the initial strain and the creep for both HSC and VHSC at stress levels less than 40 % of the strength. Stress/strength ratios larger than 40 % cause a progressive creep of the HSC and the VHSC in relation to the initial strain. The stress/initial strain relation is linear according to Fig. 9.1. The creep is not linear according to the creep coefficient in Fig. 9.3 and Fig. 9.4.

9.2 Discussion

The visco-elastic creep hypothesis requires a linear relation between stress and creep. The linear relation has been studied by a number of researchers.

Linear relation between creep and stress has been reported and the limit of linearity has been proposed to be in a range of 0.23 to 0.75 of the compressive strength. The limit of linear relation between creep and stress of HSC has been reported as 65 % of the compressive strength while the limit of NSC was reported as 40 % in the same investigation [87.3].

The linearity has in previous work been evaluated in relation to the measured creep and the stress/strength ratio. The relation between creep and stress has been proposed to be linear based upon linear regression despite of the fact that the regression lines do not pass through the origin.

The test results of this investigation reveal that linear regression lines might be drawn and apparently a linear relation between stress and strain can be observed. Further analysis by means of the specific creep and the creep coefficient reveal different relations.

A limit of linearity exist undoubtedly. The limit of linearity is related to microcracks and the limit is therefore affected by shrinkage. Increased shrinkage will decrease the limit. The presence of shrinkage cracks probably causes the large scatter in proposed limits of linearity. Ali S. Ngab [80.1] reported the limit of linearity of a HSC to 65 % of the compressive strength. Analysis of the amount of cracks revealed that the HSC did not suffer from

significant cracking caused by shrinkage or the stress/strength level. The NSC exhibited an increase in the amount of microcracks at stress levels exceeding 40 % of the compressive strength.

The VHSC investigated in this present research exhibits a highly developed microcrack pattern as reported in section 10. Even the unloaded shrinkage specimens exhibit significant microcracking.

The microcracks cause the non-linear creep-stress behavior after some time. The shrinkage cracks have not developed at the time of loading and will not cause non-linearity of the stress/initial strain relation.

9.3 The CEB-FIP modelcode 1990

The CEB-FIP approach prescribe linearity between the creep coefficient and the stress/strength ratio. The limit of linearity is at $\sigma/f_c = 0.4$. At σ/f_c ratios exceeding 0.4 CEB-FIP proposes {9.1} to account for the non-linearity.

$$\varphi = \varphi_{0.4} \cdot \mathrm{EXP}\left[1.5 \left(\frac{\sigma}{f_c} - 0.4 \right) \right] \qquad \{9.1\}$$

Equation {9.1} is illustrated in Fig. 9.2, Fig. 9.3 and Fig. 9.4 by dashed lines. The $\varphi_{0.4}$ determined by tests has been used in {9.1}. Equation {9.1} reveals a very good correlation between the test results of the HSC and the VHSC and the CEB-FIP approach. {9.1} supports the assumption that the HSC and the VHSC do not exhibit linear relation between creep and stress at stress levels exceeding 0.4.

The LSC exhibits no relation to the CEB-FIP models proposed range of applicability. The LSC reveals a linear relation between creep and initial strain in the range 0-60 % of the compressive strength but does not exhibit linear creep.

The dashed curves in Fig. 9.2 illustrating the relation between $\varphi_{0.4}$ and the CEB-FIP approach reveal that the creep coefficient at the stress/strength ratio of 75 % do not follow the same creep-time relation as the creep-time relation at the stress/strength ratio of 40 %. This is due to the development of severe cracks in the first 1400 hours and the development of strength which cause a stabilization of the crack development. See section 7.

9.4 Conclusions

1. The LSC has a creep-stress linearity limit less than 0.33 of the compressive strength. The HSC has a creep-stress linearity limit between 0.33 and 0.4 of the compressive strength while the VHSC exhibits linearity between creep and stress to a limit in the range of 0.4 and 0.5 of the compressive strength.

2. The LSC exhibits linear relation between creep and initial strain for stress/strength ratios in the range of 0 to at least 0.6 of the compressive strength.
   The HSC and the VHSC exhibit linear relation between creep and initial strain for a stress/strength ratio in the range of 0 to 0.4-0.5.

3. The CEB-FIP approach predicts the non-linearity very well for HSC and VHSC, while the LSC exceeds the range of application proposed by CEB-FIP.

4. The stress/initial strain relation is linear for the HSC and the VHSC in the stress range of 0 to at least 0.7 of the compressive strength.
   The stress/initial strain relation of the LSC is linear for stress less than 0.4 of the compressive strength.

5. The development of shrinkage cracks causes the limit of linearity and is most significant for HSC and VHSC.
   The limit of linearity is as a corollary related to the shrinkage and the mechanisms which affect shrinkage.

10 MICROCRACKING

This section is an analysis of a number of thin-sections. Microcracks in the concrete are detected by means of computer analysis. The results confirm previous conclusions related to microcracks.
The results of the analysis confirm the proposed mechanism between shrinkage and load developed microcracks.

10.1 Experimental results

The load has been removed from the sealed and unsealed LSC (3,4) and VHSC (11,12), and thin-sections have been cut from one loaded and one unloaded specimen of each test. Two thin-sections in two perpendicular planes have been cut of each specimen after a period of at least 1 year of loading and/or drying. 16 thin-sections have been made.
The microcracks have been detected by means of digital computer analysis. 3 digitized areas of 3.0 x 3.2 mm have been analyzed from each thin-section. 4 of these 48 areas are illustrated in Fig. 10.1 and Fig. 10.2. Fig. 10.1 illustrates the LSC. The thin-sections of the LSC reveal that the high porosity makes it impossible to define cracks, if there are any.
In Fig. 10.2 the VHSC is illustrated. The thin-sections reveal a highly developed crack-pattern. The cracks are both bond and mortar cracks.
Because of the high porosity of the LSC, no computer analysis has been performed on the LSC thin-sections.
In Table 10.1 are the average crack-lengths of the 24 analyzed VHSC digitized areas presented.

Table 10.1 *Average crack-length in mm of VHSC thin-sections.*

		Unloaded	Loaded
Vertical	Sealed	11.9	17.7
Horizontal	Sealed	12.7	11.0
Vertical	Unsealed	11.4	14.8
Horizontal	Unsealed	18.4	18.6

In Table 10.2 are the average values of the vertical and horizontal crack-lengths presented.

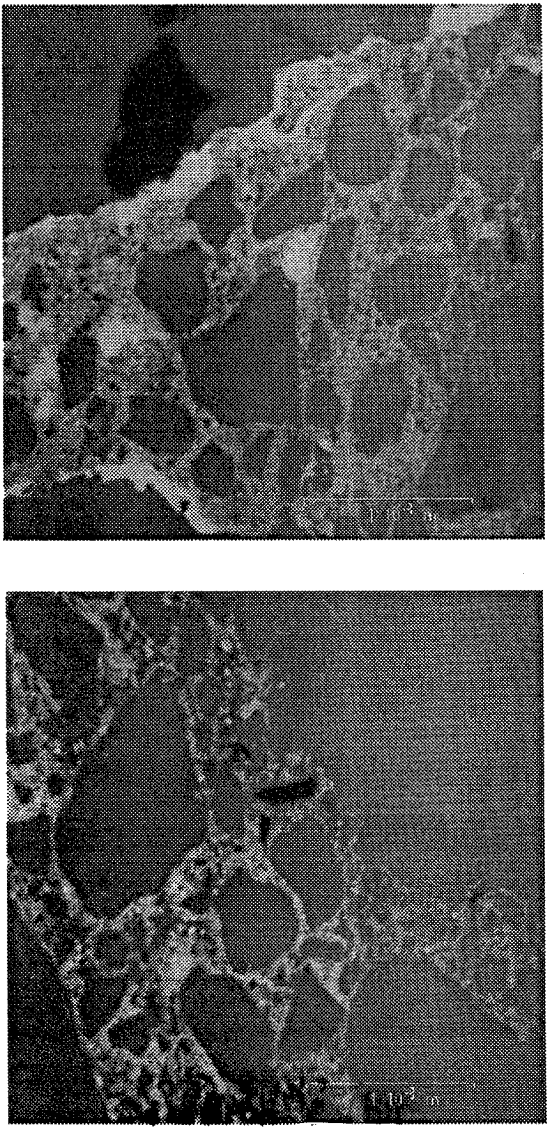

Fig. 10.1 Thin-section of LSC. Upper picture shows an unloaded specimen and the lower picture shows a loaded specimen. Scale : 10^{-3} m.

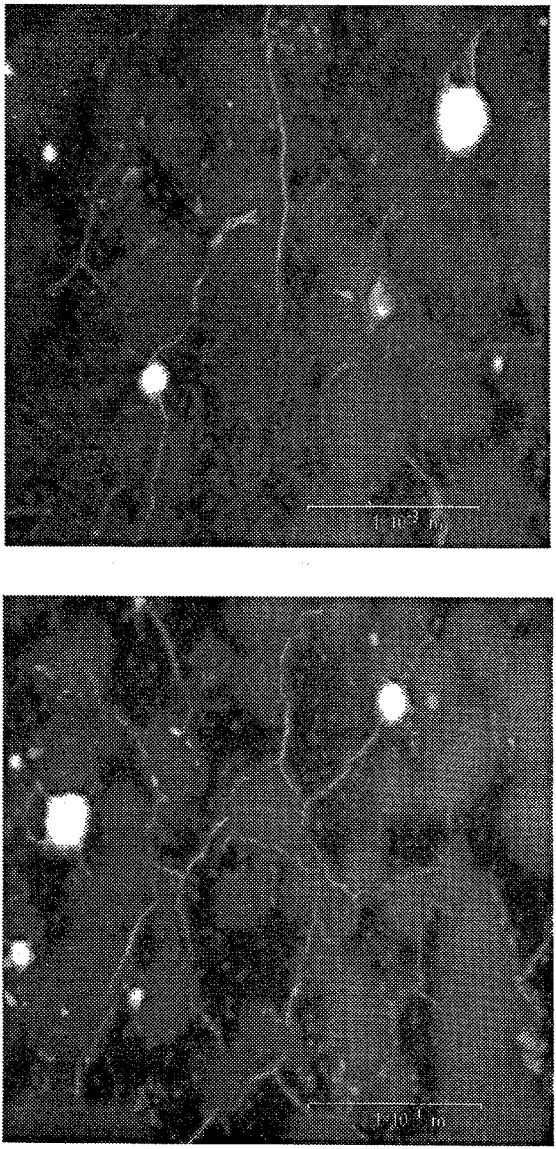

Fig. 10.2 Thin-sections of VHSC. Upper picture shows an unloaded specimen and lower picture shows a loaded specimen. Scale : 10^{-3} m.

10.2 Discussion

Before any analysis of the test results are conducted, it must be emphasized that the number of specimens and analyzed digitized areas of each thin-section is rather small and any conclusions must be considered as an indication, not a rigorous fact.
Having the mentioned considerations in mind, the results in Table 10.2 confirm the influence of microcracking discussed in previous sections.

Table 10.2 *Average crack-length in mm of horizontal and vertical thin-sections.*

	Unloaded	Loaded
Sealed	12.3	14.3
Unsealed	14.9	16.7

The application of load increases the total length of microcracks. The increased shrinkage due to drying causes an increase of the total length of microcracks.
The presence of microcracks in the VHSC confirms the following subjects discussed in previous sections.

1. The offset value between creep of paste and creep of concrete.
2. The non-linearity of creep.
3. Drying shrinkage and subsequent drying creep.

The reduced shrinkage of the VHSC would lead one to believe that shrinkage does not cause microcracking. The microcracking related to shrinkage in the VHSC is due to the reduced creep.
As the paste shrinks, the restraint caused by the aggregate causes tensile stresses in the paste, which are relieved by creep. As the creep are decreased when the compressive and tensile strength are increased, then decreased shrinkage still might cause microcracking.

10.3 Conclusions

1. Despite of reduced shrinkage of the VHSC, microcracking occurs due to the reduced creep.

2. The detection of microcracks in the VHSC confirms previous conclusions related to microcracking.

11 DRYING CREEP

The drying creep is analyzed in this section in relation to the drying shrinkage and the related crack mechanism.
The analysis is based upon a mathematical fit of the test results.

11.1 Experimental results

Based upon the mathematical fitted values in section 4 and 5, the drying shrinkage and drying creep are determined. The mathematically determined drying strains are illustrated in Fig. 11.1 and Fig. 11.2.

The drying shrinkage in Fig. 11.1 are observed to be positive during the entire shrinkage period for both LSC (mix 2), HSC (mix 5) and VHSC (mix 6).

Drying creep of the LSC is positive during the entire creep period. Drying creep of the HSC and the VHSC become negative after some time. The sign of the drying creep of the HSC and the VHSC change at different times, but at the same amount of drying shrinkage.

11.2 Discussion

At least 3 factors cause drying creep.

1. Carbonation
2. Seepage
3. Microcracking

Carbonation is only observed in the LSC and is according to Parrot [75.3] negligible for specimens with a surface/volume ratio $> 15\ m^{-1}$. The specimens investigated in this research have a surface/volume ratio of $40\ m^{-1}$. Carbonation is in the following therefore assumed to be of no significance in relation to drying creep.

Drying creep is then related to seepage and microcracking. The two mechanisms act differently. Creep caused by seepage can be considered as a stress induced shrinkage, while creep related to microcracking is shrinkage induced creep, see section 1.

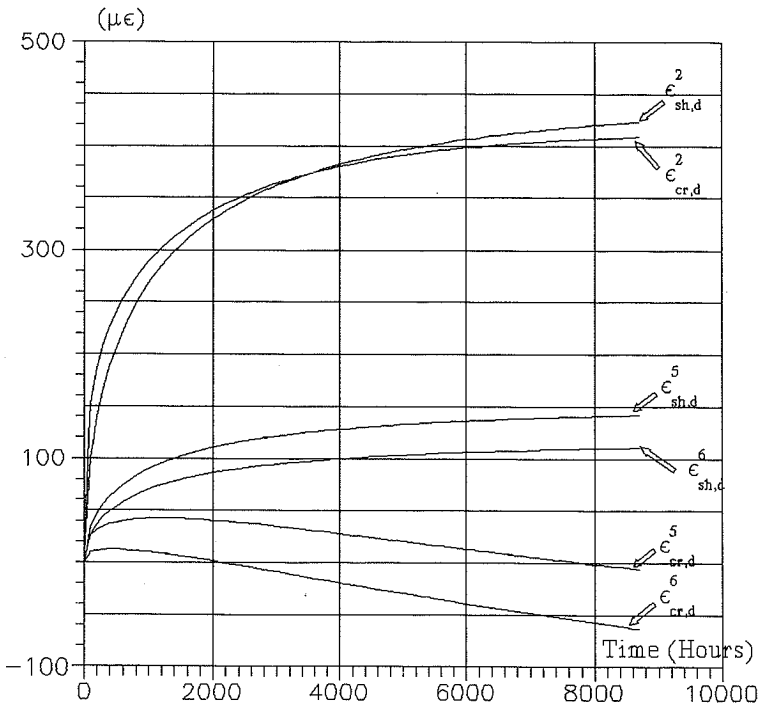

Fig. 11.1 Drying shrinkage and drying creep of LSC (2), HSC (5) and VHSC (6) in relation to time.

Creep related to microcracking caused by shrinkage is most significant in the first period after applying the load. Shrinkage develops rapidly just after applying the load in this research, because the specimens are exposed to drying at the same time. When the shrinkage rate decreases the development of microcracks stops.

Sealed specimens contain more evaporable water than unsealed specimens. Creep related to seepage is larger the more evaporable water left in the concrete.

Microcracking and seepage can explain the behavior of mix no. 5 and 6.

After applying the load and subsequent drying, microcracking contributes to creep and is most significant under drying and subsequent increased shrinkage, which causes a positive drying creep. After some time the shrinkage rate decreases and microcracking stops. The drying creep related to microcracking is now constant, creep rate equal zero. The sealed specimens

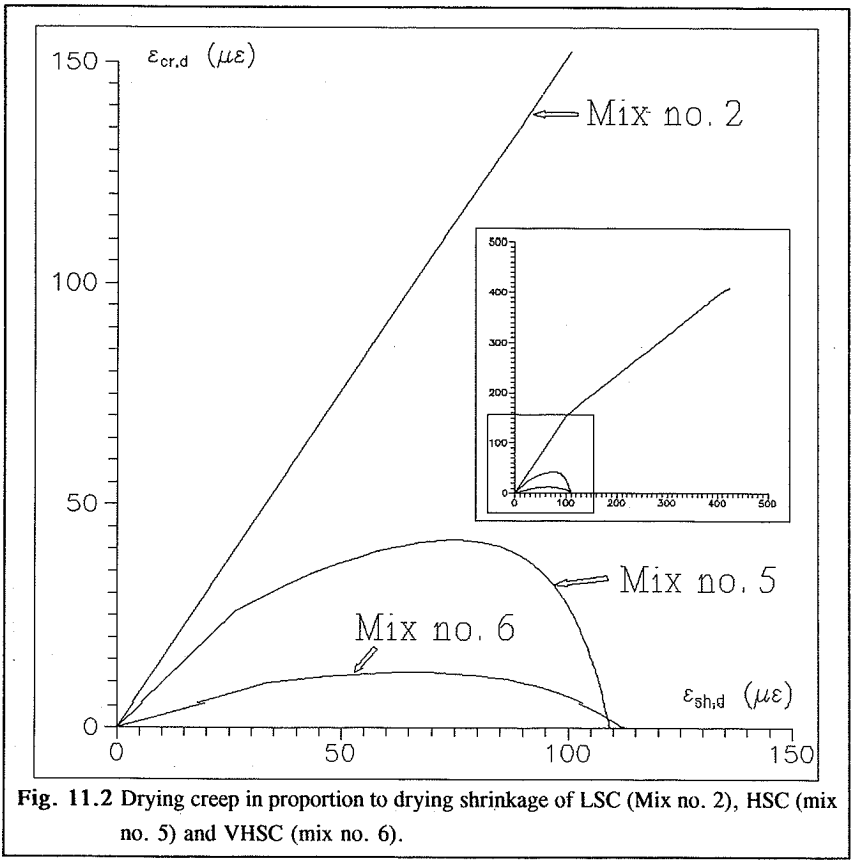

Fig. 11.2 Drying creep in proportion to drying shrinkage of LSC (Mix no. 2), HSC (mix no. 5) and VHSC (mix no. 6).

now contain more evaporable water and creep more than the unsealed specimens due to seepage. This causes a negative drying creep rate which after some time causes negative drying creep. The same behavior might be observed in Fig. 11.1 for the LSC. The drying creep related to microcracking is much more significant due to the larger drying shrinkage and the smaller tensile strength. As the shrinkage rate decreases the seepage creep causes the change in drying creep rate related to the shrinkage in Fig. 11.2. Because of the large microcrack creep, seepage creep does not cause negative drying creep in the next couple of years, if ever, for LSC.

Negative drying creep has been observed by Meyers [67.1] for NSC and for HSC by Ali S. Ngab [80.1]. However, it must be emphasized that the drying creep strains of the HSC and the VHSC in Fig. 11.1 and Fig. 11.2 are small in relation to the accuracy of the determina-

tion of strains (20 $\mu\epsilon$) and the fact that drying strains are determined by means of two different batches of the same mix.
The LSC exhibits drying creep closely related to the corresponding drying shrinkage as suggested by Kesler & Ali and Neville in section 1 {1.4} to {1.6}.

11.3 Conclusions

1. Drying shrinkage of LSC, HSC and VHSC are positive during the entire shrinkage period.

2. LSC exhibits positive drying creep during the whole creep period. HSC and VHSC exhibit positive drying creep in a period just after loading and subsequent drying and after some time drying creep becomes negative.
   It has to be emphasized that the drying creep is determined by fitted test results. The 1 year drying creep in section 5 is zero.

3. Drying creep of the LSC is closely related to the drying shrinkage as suggested by Kesler & Ali and Neville and as proposed in this research drying shrinkage causes microcracking.

12 STATIC-FATIGUE

Even though no test results concerning static-fatigue are published in the test report, the results of some pilot tests are presented in this section.
The influence of shrinkage, the development of mechanical properties and the age at application of load are discussed in relation to static-fatigue.

12.1 Experimental results

In the test-report [92.1] no test results concerning static-fatigue are presented. The load-procedure in relation to static-fatigue testing can be conducted in two different ways. The most convenient and most true load-procedure (procedure A) is to apply the load with a constant loading rate and then keep a sustained load until failure. This load-procedure was used in this investigation.

The time before failure varied from few seconds to several days. When static-fatigue failure did not occur in the first few minutes, then no failure took place. M.M. Smadi [83.1] observed the same behavior. M.M. Smadi increased the load after some time until failure. The result of Smadi's load-procedure was a decreased failure load and an increased failure strain in relation to the short-time load.
The test results of M.M. Smadi was not confirmed by this investigation. Sometimes the failure load was increased in relation to the short-time failure load and some times it was decreased.

The other load-procedure (procedure B) is to decrease the loading rate for different specimens. The two load-procedures are illustrated in Fig. 12.1.

12.2 Discussion

Even though no specific static-fatigue tests have been performed, the test results discussed in previous sections behave in a way which without any doubt will influence the static-fatigue strength. Some of these factors are

1. Shrinkage and subsequent microcracking.
2. Development of strength.

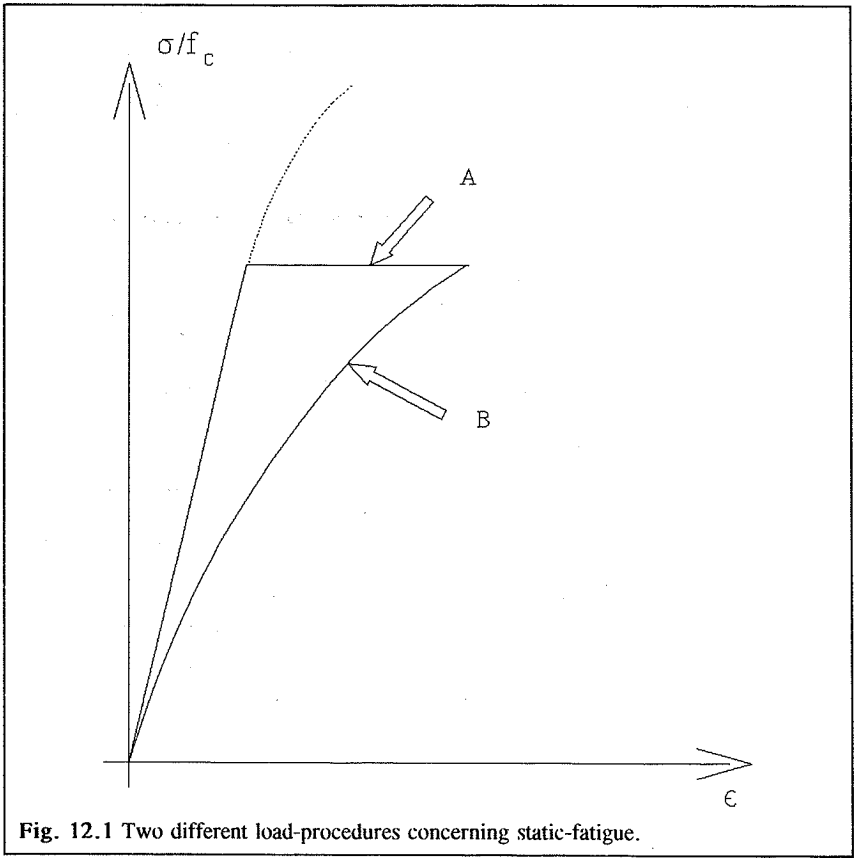

Fig. 12.1 Two different load-procedures concerning static-fatigue.

Failure is related to micro- and macrocracking. Theoretically, a loaded concrete specimen can be in a stable state of micro/macrocracking just at the static-fatigue limit. At this stable state of cracking an infinite crack development will cause static-fatigue failure. Shrinkage related to drying or selfdesiccation might cause microcracks as pointed out in previous sections. A corollary is that static-fatigue failure is dependent on shrinkage and drying. Norwegian dynamic-fatigue tests have revealed that the dynamic-fatigue failure is dependent on the environmental conditions.

If static-fatigue failure is dependent on shrinkage then static-fatigue failure is also dependent on the age at loading and the age at loading after drying has begun.

The influence of the development of strength and stiffness has been underlined in section 7.

The development of strength is also related to the age at loading and the environmental conditions.

Shrinkage and the development of strength affects the static-fatigue strength more significantly if static-fatigue failure does not occur within the first week after loading.

12.3 Conclusions

1. Static-fatigue failure is dependent on the development of micro/macrocracking caused by shrinkage. The static-fatigue strength is dependent on the environmental conditions in the extent of the influence on shrinkage.

2. Static-fatigue strength is dependent on the development of strength and stiffness.

3. The age at application of load affects shrinkage and the development of strength and as a corollary the static-fatigue strength is related to the age at application of load.

13 CREEP RECOVERY

This section deals with the recovery creep of LSC, HSC and VHSC. The recovery creep is analyzed in relation to the weight-loss and the development of stiffness.

13.1 Experimental results

After approximately 6800 hours (280 - 290 days) the LSC (29), the HSC (28) and the VHSC (27) have been unloaded and the creep recovery strains have been determined. The specific creep strains are illustrated in Fig. 13.1.
The initial strain at unloading and the initial strain at loading of 3 companion specimens are presented in Table 13.1. The companion specimens were loaded until failure at the same day as the unloading took place.

Table 13.1 *Initial strains in $\mu\varepsilon$ at unloading and loading from/to the same stress.*

	LSC (2)	HSC (28)	VHSC (27)
Unloading (A)	190	603	683
Loading (B)	200	673	764
A/B	0.95	0.90	0.89

Approximately 2000 hours (80 days) after the concrete specimens have been unloaded, the creep recovery in relation to the specific creep just before unloading is 6.1 % for the LSC, 28.6 % for the HSC and 33.7 % for the VHSC.
In Fig. 13.1 the levels corresponding to the initial loading strain at the time of unloading are illustrated.
The outlined levels of the initial loading reveal that the LSC, the HSC and the VHSC recover more than just the initial loading strain.

13.2 Discussion

A large number of tests on mortars performed by Neville [60.1] reveal that an increased

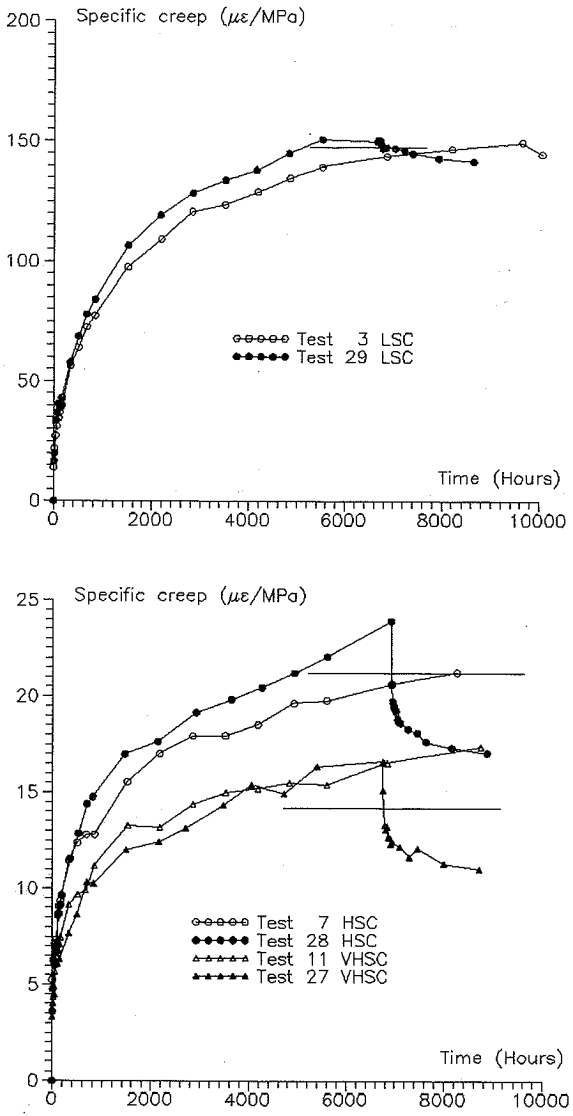

Fig. 13.1 Specific creep and specific creep recovery of LSC, HSC and VHSC.

compressive strength increases the recovery creep/creep ratio.
The present tests confirm this behavior for concretes with compressive strength ranging from 15 MPa to 100 MPa.
Meyers [67.1] and Staley & Peabody [46.1] concluded, based on experimental results, that the older the concrete is at application of load the higher creep recovery/creep ratio.
On the contrary, Illston [65.2] and Ishai [64.2] found that the creep recovery is independent on the age at application of load and the time under sustained load.
According to the stated hypothesis relating microcracking to shrinkage stress and external stress discussed in previous sections, the time under load with no doubt affects the amount of recoverable creep.
As shrinkage is dependent on the age at drying and microcracking is related to shrinkage, then microcracking is dependent on the load age and time of drying and as a corollary, recovery creep is dependent on the age at loading and time under sustained load.
Considering recovery creep as related to the same mechanism which cause creep, then aging affects the recovery creep related to the age at loading and the time under load.

Applying a load to a concrete specimen which is in hydrostatic equilibrium and which does not hydrate anymore does not cause creep, as long as no cracks are developed.
A concrete specimen which is unloaded after hydration has stopped and the specimen has reached hydrostatic equilibrium is not supposed to recover or at least the recovery is expected to be significantly reduced in relation to unloading before hydration/drying have stopped.
According to the weight-loss and strength development of the LSC, the concrete is in a stable state at unloading and the recovery is as expected significantly reduced in relation to the recovery of the HSC and the VHSC.
The HSC and the VHSC have not reached hydrostatic equilibrium at the time of unloading and exhibit a larger amount of recovery than the LSC.

13.3 Conclusions

1. The recovery creep/creep ratio is increased as the compressive strength is increased.

2. Based upon indirect results it must be concluded that the recovery creep is dependent on the age at loading and the time under load.

3. Creep and the recovery creep are correlated to the weight-loss.

14 EFFECTS OF CREEP

This section is a brief review of the effects of creep in general and the consequence on these subjects in relation to the achieved results.

Table 14.1 *Effects of creep*

Beneficial	Harmful
1. Relif of stress concentrations induced by shrinkage, temperature changes etc.	1. Creep buckling of columns 2. Loss of pre-stress

The effect of the creep of concretes with high strength affect the subjects in Table 14.1.

A reduced creep decreases the beneficial effect of creep causing a relif of restraining stresses. The reduced shrinkage of concretes with high strength cause less restrain. Due to the reduced restrain the beneficial effect of creep might not be affected by an increase of the compressive strength as far as shrinkage is concerned.

A reduced creep decreases the harmful effects of creep.

14.1 Conclusions

1. Considering the subjects investigated in this report, high strength concrete is in general a material with improved mechanical time-dependent properties.

15 FINAL CONCLUSIONS

1. Concretes with high strength up to 100 MPa do not exhibit any discrepancy in relation to the known mechanisms of concrete shrinkage and creep.
   Concretes with high compressive strength, containing micro silica fume, fly-ash and/or plasticizer, are not a new material with respect to the time-dependent mechanical properties of shrinkage, creep and strength/stiffness development.

2. Microcracks have an important influence on creep but do not explain the total amount of creep.
   A large amount of the drying creep is probably related to microcracking caused by an interplay between shrinkage and applied stress.

3. The performed tests confirm that water in the concrete is the main reason for shrinkage and creep.
   As high strength concrete contains less water and has a denser structure the time-dependent properties are less significant.

4. Even though it is not the scope of this investigation, it can be concluded that the CEB-FIP modelcode 1990 in general correlates well to the mechanisms concerning the time-dependent mechanical properties of the investigated concretes.
   It must be emphasized that the investigated concretes, as high performance concretes, exceed the range of applicability of the CEB-FIP modelcode 1990.

16 REFERENCES

[26.1] The effect of varied curing conditions upon the compressive strength of mortars and concretes
Herbert J. Gilkey
Procedings of the American Concrete Institute, Vol. 22, 1926, pp. 395-436.

[30.1] Studies on reinforced concrete, III: The creep or flow of concrete under load
W.H. Glanville
Building Research Technical Paper No. 12. Departement of Scientific and Industrial Research: London 1930

[32.1] Plain and reinforced concrete arches
C.S. Whitney
ACI Journal, 28, 1932, pp. 479-519

[37.1] Untersuchungen über die Knicksicherheit, die elasticher Verformung und das Kriechen des Betons bei Bogenbrüchen
F. Dischinger
Der Bauingenieur, 18, No. 33/34, 1937, pp. 487-520; No. 35/36, 1937, pp. 539-552; No. 39/40, 1937, pp. 595-621.

[41.1] Concrete under sustained working loads; evidence that shrinkage dominates time yield
G. A. Maney
Proc. ASTM, 41, 1941, pp. 1021-1030

[46.1] Shrinkage and plastic flow of prestressed concrete
H.R. Staley and D. Peabody
ACI Journal, 42, 1946, pp. 229-243

[51.1] Factors Influencing Concrete Strength.
Walter H. Price
Journal of the American Concrete Institute, February 1951, pp. 417-432.

[56.1] Effect of aggregate on shrinkage of concrete and a hypothesis concerning shrinkage.
G. Pickett
Journal of the American Concrete Institute, 52, (1956), pp. 581-590.

[58.1] Geoteknik.
H. Lundgren, J. Brinch Hansen
Teknisk Forlag, København 1958, kap. 1.2- 1.3, 19-43

[59.1] Role of cement in the creep of mortar
A.M. Neville
ACI Journal, 55, 1959, pp. 963-984.

[59.2] Étude sur fluage du béton
M. Mamillan
Annales Institut Technique du Batiment et des Travaux Publics, No. 134, Paris, Fe. 1959, pp. 221-233.

[59.3] Causes and control of volume change.
T.C. Powers
J. Portl. Cem. Assoc. Research and Development Laboratories, 1, No.1, pp. 29-39, 1959.

[60.1] Recovery of creep and observations on the mechanism of creep of concrete
A.M. Neville
Appl. Sci. Res.,9, 1960, pp. 71-84

[62.1] Modulus of elasticity of concrete affected by elastic moduli of cement paste matrix and aggregate
T.J. Hirsch
ACI Journal, 59, 1962, pp. 427-451

[62.2] Discussion on "Modulus of elasticity of concrete affected by elastic moduli of cement paste matrix and aggregate"
J.W. Dougill
ACI Journal, 59, 1962, pp. 1363-1365

[63.1] Microcracking of plain concrete and the shape of the stress-strain curve.
Thomas T.C. Hsu, Floyd O. Slate, Gerald M. Sturman and George Winter.
ACI Journal, february 1963, pp. 209-223.

[64.1] Creep of concrete as a function of its cement paste content.
A.M. Neville.
Magazine of concrete research, Vol. 16, No. 46, March 1964, pp. 21-30.

[64.2] Elastic and inelastic behavior of cement mortar in torsion
O. Ishai
American Concrete Institute Special Publication No. 9, 1964, pp. 65-94

[64.3] The effect of the elastic modulus of the aggregate on the elastic modulus, creep and creep recovery of concrete.
U.J. Counto
Magazine of Concrete Research, 16, No. 48, 1964, pp. 129-138

[64.4] Mechanisms of creep in concrete
C.E. Kesler and I. Ali
Symposium on creep of concrete, SP-9 American Concrete Institute, Detroit , 1964, pp. 35-63.

[65.1] Methods of computing stress in concrete from from a history of measured strain
G.L. England and J.M. Illston
Civil Engineering and Public Works Review, 60, 1965: No. 705, pp. 513-517; No. 706, pp. 692-694; No. 707, pp. 846-847.

[65.2] The components of strain in concrete under sustained compressive stress
J.M. Illston
Magazine of Concrete Research, 17, No. 50, 1965, pp. 21-28

[67.1] Time-dependent strains and microcracking of plain concrete
B.L. Meyers.
PhD Thesis, Cornell University, Ithaca, New York, 1967.

[68.1] Elementær statistik og sandsynlighedsregning; Bind 1.
Poul Aarøe
Polyteknisk Forlag, 1968.

[69.1] Relationship between time-dependent deformation and microcracking of plain concrete
Bernard L. Meyers, Floyd O. Slate and George Winter.
ACI Journal , January 1969, pp. 60-68

[69.2] Physical and chemical causes of creep and shrinkage of concrete.
RILEM symposium, Munich, April 1-3, 1968.
Materials and structures, Vol.2, No.8, March-April 1969.

[70.1] Some factors influencing the long term strength of concrete.
B.P. Hughes and J.E. Ash.
Materials and Structures, Vol. 3, No. 14, 1970, pp. 81-84.

[72.1] Rheology of building materials.
Anders Nielsen
National Swedish Building Research, 1972.

[75.1] Criteria and designs for creep apparatus.
B.R. Gamble.
Concrete, December 1975, pp. 26-27,37.

[75.2] Estimating long-term creep and shrinkage from short-term tests.
J.J. Brooks and A.M. Neville
Magazine of Concrete Research: Vol.27, No. 90: March 1975. pp. 3-12

[75.3] Increase in creep of hardened cement paste due to carbonation under load.
L.J. Parrott.
Magazine of Concrete Research: Vol.27, No.92: September 1975. pp. 179-181

[75.4] Moisture state for a standard creep test.
L.J. Parrott.
Concrete, December 1975, pp. 25-26.

[75.5] Recommendations for a standard creep test.
J.M. Illston and C.D. Pomeroy.
Concrete, December 1975, pp. 24-25.

[75.6] The strength and deformation characteristics of high early strength structural concrete
R.N. Swamy, A.B. Ibrahim, K.L. Anand
Materials and structures, Vol.8 No. 48, 1975, pp. 413-423

[75.7] Time-dependent behavior of concrete containing a plasticiser
A.M. Neville and J.J. Brooks
Concrete Vol 9. 1975, pp. 33-35

[76.1] Measurement of deformation under compressive load.
CPC-12.
Materials and Structures, Vol. 9, No. 52, 1976, pp. 43-48

[76.2] Creep of fly ash concrete
R.P Lohtia, B.D. Nautiyal and O.P. Jain
ACI Journal, august 1976, pp. 469-472

[77.1] A low-cost creep rig for concrete.
L. Cridland, S.L. Bakoss and A.J. Burfitt.
Magazine of concrete research, Vol. 19, No. 100, September 1977, pp. 147-150

[79.1] Time-dependent properties of concrete containing a superplasticizing admixture.
J.J. Brooks, P.J. Wainwright and A.M. Neville.
ACI SP 62-15, 1979, pp. 293-314

[80.1] Behavior of high-strength concrete under sustained compressive stress.
Ali Salem Ngab
PhD Thesis, Cornell University, 1980.

[80.2] Microcracking and engineering properties of high-strength concrete.
Ramon Luis Carrasquillo.
PhD Thesis, Cornell University, 1980.

[81.1] Creep of fly ash concrete.
Ram S. Ghosh and John Timusk.
ACI Journal, September-October 1981, pp. 351-357.

[81.2] Microcracking and time-dependent strains in high strength concrete
Ali S. Ngab, Floyd O. Slate and Arthur H. Nilson
ACI journal, july-august 1981, pp. 262-268

[81.3] Microcracking and behavior of high strength concrete subjected to short-term loading.
Ramon L. Carrasquillo, Floyd O. Slate and Arthur H. Nilson.
ACI Journal, May-June 1981, pp. 179-186.

[81.4] Shrinkage and creep of high strength concrete
Ali S. Ngab, Arthur H. Nilson and Floyd O. Slate
ACI Journal, july-august 1981, pp. 255-261

[81.5] Time-dependent behavior of high-early-strength concrete containing a superplasticizer.
J.J. Brooks, P.J. Wainwright and A.M. Neville.
ACI SP 68-5, 1981, pp. 81-100

[81.6] Properties of Concrete, 3rd Edition
A.M. Neville
Pitman, 1981

[82.1] Standard test method for creep of concrete in compression.
ASTM. Designation: C 512-76.
Annual Book of ATSM Standards, Part 14. 1982 pp. 341-345.

[83.1] Time-dependent behavior of high-strength concrete under high sustained compressive stresses.
Mohammad Mahmoud Smadi.
PhD Thesis, Cornell University, 1983.

[83.2] Mechanical properties, durability and drying shrinkage of portland cement concrete incorporating silica fume.
Georges G. Carette and V. Mohan Malhotra.
Cement, Concrete, and Aggregates, Vol. 5, No. 1, Summer 1983, pp. 3-13.

[83.3] Microcracking and definition of failure of high- and normal-strength concretes.
Ramon L. Carrasquillo and Floyd O. Slate.
Cement, Concrete, and Aggregates, Vol. 5, No. 1, Summer 1983, pp. 54-61.

[83.4] Properties of ultra-high-strength concrete containing a superplasticizer.
J.J. Brooks and P.J. Wainwright.
Magazine of concrete research, Vol. 35, No. 125, December 1983, pp. 205-213.

[83.5] Shrinkage and creep of mass concrete containing fly ash.
Takeshi Yamato and Hideaki Sugita.
ACI SP 79-4, 1983, pp. 87-102.

[83.6] Superplasticized high-workability concrete: some properties in the fresh and hardned states.
Ravindra K. Dhir and Andrew W.F. Yap.
Magazine of concrete research, Vol. 35, No. 125, December 1983, pp. 214-228.

[83.7] Creep of plain and structural concrete.
A.M. Neville, W.H. Dilger and J.J. Brooks.
Construction Press, New York 1983. pp. 1-351.

[84.1] Accuracy of estimating long-term strains in concrete.
J.J. Brooks
Magazine of concrete research, Vol. 36, No. 128, September 1984, pp. 131-145

[84.2] State-of-the-art report on high-strength concrete
ACI Committee 363
ACI Journal, july-august 1984, pp. 383-389

[84.3] Superplasticized flowing concrete: strength and deformation properties.
Ravindra K. Dhir and Andrew W.F. Yap
Magazine of concrete research, Vol 36, No. 129, December 1984, pp. 203-215

[84.4] Ultra high-strength field placeable concrete with silica fume admixture.
John Wolsiefer.
Concrete International, April 1984, pp. 25-31.

[84.5] Dansk Ingeniørforenings norm for betonkonstruktioner
Normstyrelsens publikationer
Teknisk forlag, 3.udg., 1984

[84.6] Fatigue and microcracking of concrete.
Thomas T.C. Hsu
Materials and Structures, Vol. 17, No. 97, 1984, pp. 51-54

[84.7] Practical prediction of creep and shrinkage of high strength concrete
Zdenek P. Bazant, Liisa Panula
Materials and Structures, Vol. 17 No. 101, 1984, pp. 375-378

[85.1] A modified absorption theory.
Arne Hillerborg.
Cement and Concrete Research, Vol. 15, 1985, pp. 809-816.

[85.2] Creep of a silica concrete.
M. Buil, P. Acker.
Cement and concrete research. Vol 15, 1985, pp. 463-466

[85.3] High-, medium-, and low-strength concretes subjected to sustained overloads-strains, strength and failure mechanisms
Mohammad M. Smadi, Floyd O. Slate and Arthur H. Nilson
ACI journal, september-october 1985, pp. 657-664

[85.4] High-strength concrete - Material properties and structural behavior.
R.N. Swamy
ACI SP-87-8, 1985, pp. 119-146.

[85.5] Høyfast betong. Delrapport 5. Pilotforsøk med kryp i høyfast betong.
A. Tomaszewics
SINTEF rapport, STF65 A85006, 1985, pp. 1-18

[85.6] Mass transfer of water through concrete.
R.H. Mills.
Cement and Concrete Research, Vol. 15, 1985, pp. 74-82.

[85.7] Mechanical properties of high strength concretes based on different binder combinations
Vesa Penttala
ACI SP 87, 1985, pp. 123-134

[85.8] Betonbogen
AA. D. Herholdt mfl.
Aalborg, Cementfabrikkernes tekniske Oplysningsråd, 2.udg. 1985.

[86.1] A 4:1 range in concrete creep when cement SO_3 content, curing temperature and fly ash content are varied.
K.M. Alexander, J. Wardlaw and I. Ivanusec.
Cement and Concrete Research, Vol 16, 1986, pp. 173-180.

[86.2] Creep of concrete containing fly ash and superplastcizer at different stress/strength ratios.
K.W. Nasser and A.A. Al-Manaseer.
ACI Journal, July-August 1986, pp. 668-673.

[86.3] Drying shrinkage and creep of concrete with condensed silica fume
E. Tazawa and A. Yonekura
ACI SP 91-43, 1986, pp. 903-921

[86.4] Field study of creep and shrinkage of a very high strength concrete
P. Laplante and P.C. Aitcin
Fourth int. RILEM conference, 1986, Northwestern University, pp. 777-786

[86.5] Properties of high-strength concrete
Ramnath N. Swamy
Cement, Concrete and Aggregates, Vol. 8, No. 1, 1986, pp. 33-41

[86.6] Handbook of Chemestry and Physics.
Chemical Rubber Publishing Company
1986-1987

[86.7] Shrinkage and creep of concrete containing 50 percent lignite fly ash at different stress-strength ratios.
K.W. Nasser and A.A. Al-Manaseer.
ACI SP 91-20, 1986, pp. 433-448.

[87.1] Measurement of internal concrete strains using embedment strain gauges
R.H. Scott and P.A.T. Gill
Magazine of concrete research, Vol. 39, No. 139, June 1987, pp. 109-112

[87.2] Microcracking of concrete under compression and its influence on tensile strength.
A. Delibes Liniers
Materials and Structures, 1987, 20, 111-116

[87.3] Shrinkage and creep of high-, medium-, and low-strength concretes, including overloads.
Mohammad M. Smadi, Floyd O. Slate and Arthur H. Nilson
ACI materials journal, may-june 1987, pp. 224-234

[87.4] Shrinkage and creep of concrete containing 50% lignite fly ash at high temperatures.
Karim W. Nasser and Akthem A. Al-Manaseer.
Cement, Concrete, and Aggregates, Vol. 9, No. 2, Winter 1987, pp. 95-100.

[87.5] Silica fume in high-strength concrete.
V. Yogendran, B.W. Langan, M.N. Haque and M.A. Ward.
ACI Materials Journal, March-April 1987, pp. 124-129.

[87.6] Silica fume in concrete.
ACI Committee 226.
ACI Materials Journal, March-April 1987, pp. 158-166.

[87.7] Statistical extrapolation of shrinkage data-Part II: Bayesian updating.
Z.P. Bazant, J.K. Kim, F.H. Wittmann and F. Alou
ACI Materials Journal, March-April 1987, pp. 83-91

[87.8] Statistical extrapolation of shrinkage data-Part I: Regression
Z.P. Bazant, J.K. Kim, F.H. Wittmann and F. Alou
ACI Materials Journal, Januaru-February 1987, pp. 20-34

[87.9] Statistics of shrinkage test data.
Folker H. Wittmann, Zdenek P. Bazant, Fermin Alou and Jin-Keun Kim.
Cement, Concrete, and Aggregates, Vol. 9, No. 2, Winter 1987, pp. 129-153.

[88.1] Condensed silica fume in concrete
FIP State of the art report
Thomas Telford, London, 1988, pp. 1-19

[88.2] High-strength structural concrete. Materials and mechanical properties.
Ivar Holland.
Nordisk betong, 1988, 2-3, pp. 55-61.

[88.3] Høyfast betong
Odd E. Gjørv
Nordisk Betong, 1988, 1, pp. 5-9

[89.1] A model for the non-linear time-dependent behavior of concrete in compression based on a maxwell chain with exponential algorithm.
I. Carol and J. Murcia
Materials and structures, 1989, 22, pp. 176-184.

[89.2] Influence of mix proportions, plasticizers and superplasticizers on creep and drying shrinkage of concrete
J.J. Brooks
Magazine of Concrete Research, 1989, 41, No. 148, September, pp. 145-153

[89.3] Mechanical properties of high-strength concrete
Markus Held
Darmstadt Concrete, Vol. 4 1989, pp. 71-79

[89.4] Prediction of concrete drying shrinkage from short-term measurements.
Jamal A. Almudaiheem and Will Hansen.
ACI Materials Journal, July-August 1989, pp. 401-408.

[89.5] Properties of high-strength concrete with silica fume using high-range water reducer of slump retaining type.
K. Mitsui, H. Kasami, Y. Yoshioka and M. Kinoshita.
ACI SP 119-4, 1989, pp. 79-97.

[89.6] Proportioning high-strength concrete to control creep and shrinkage
Therese M. Collins
ACI Materials Journal, November-december 1989, pp. 576-580

[89.7] Sensitivity analysis of concrete prediction formulas for creep and shrinkage of concrete.
Tatsuya Tsubaki.
Transactions of the Japan Concrete Institute, Vol. 11, 1989, pp. 97-104.

[89.8] Shrinkage and creep in certain high performance concrete for use in site.
Michel Auperin
Research department Bouygues, 1989, pp. 1-39

[89.9] Preliminary data on long-term strength development of condensed silica fume concrete.
G.G. Carette
Third international conference on fly ash, silica fume, slag and natural pozzolans in concrete, Trondheim, supplementary papers, pp 597-617, 1989.

[90.1] Concrete Technology
A.M. Neville & J.J. Brooks
Longman Scientific & Technical, 1990.

[90.2] Further modification of the Ross equation to predict the ultimate drying shrinkage of concrete.
Faisal H. Al-Sugair and Jamal A. Almudaiheem.
ACI Materials Journal, May-June 1990, pp. 237-240.

[90.3] Long-term characteristics of a very high strength concrete
P.C. Aitcin, S.L. Sarkar, P. Laplante
Concrete International, january 1990, pp. 40-44

[90.4] Microporosity, creep and shrinkage of high-strength concretes
V. Penttala and T. Rautanen
ACI SP 121-21, 1990, pp. 409-432

[90.5] Mikrorevner i tæt silicabeton.
Hans Henrik Bache
Dansk Beton, nr. 4, 1990, pp. 9

[90.6] The statistical distribution of the drying shrinkage of concrete using Monte Carlo simulation.
F.H. Al-Sugair and J.A. Almudaiheem.
Magazine of concrete research, 1990, 42, No. 151, Jun, pp. 97-103.

[90.7] CEB-FIP Model Code 1990.
Bulletin d'information No 196
CEB Comite Euro-International du Beton

[90.8] Creep and shrinkage of high-strength field concretes.
Francois de Larrard.
ACI SP-121-28, 1990, pp. 577-598

[91.01] On the long-term strength losses of silica-fume high-strength concretes.
F. de Larrard and J.-L. Bostvironnois
Magazine of Concrete Research, 1991, 43, No. 155, pp. 109-119.

[91.02] State-of-the-art rapport for Højstyrkebetons svind og krybning.
Henrik Elgaard Jensen
Afdelingen for Bærende Konstruktioner, Danmarks tekniske Højskole, 1991.

[91.03] State-of-the-art rapport for Revnet betons styrke.
Henrik Elgaard Jensen
Afdelingen for Bærende Konstruktioner, Danmarks tekniske Højskole, 1991.

[91.04] Silica Fume Concrete in Melbourne, Australia.
Ian Burnett
Concrete International, August 1991, pp. 18-24.

[91.05] Betons krybning og stivhed
Lauge Fuglsang Nielsen
Laboratoriet for bygningsmaterialer, Danmarks tekniske Højskole, 1991.

[91.06] Selvudtørringssvind i mørtel og beton.
Mikkel Knudsen & Niels Gottlieb.
Laboratoriet for bygnings materialer, Danmarks tekniske Højskole, 1991.

[91.07] Role of Aggregate in the shrinkage of Ordinary Portland and Expansive Cement Concrete.
Mitsuru Saito, Mitsunori Kawamura & Seiichi Arakawa.
Cement & Concrete Composites 13 (1991) pp. 115-121.

[91.08] Selvudtørringssvind i højstyrkebeton med lavt v/c-forhold.
Pernille Forsberg, Bjarne Rasmussen
Danmarks Ingeniørakademi B, Fysik & Materialer, 1991.

[91.09] Improved prediction model for time-dependent deformations of concrete: Part 1 - Shrinkage.
Zdenek P. Bazant, Joong-Koo Kim
Materials and Structures, 1991, 24, 327-345.

[91.10] Consequences of diffusion theory for shrinkage of concrete.
Zdenek P. Bazant, Joong-Koo Kim
Materials and Structures, 1991, 24, 323-326.

[91.11] The contradiction of applying the superposition principle for concrete creep.
Jing Hua Shen, Joost C. Walraven.
Darmstadt Concrete Vol.6, 1991, pp. 65-75.

[91.12] Improved prediction model for time-dependent deformations of concrete: Part 2 - Basic creep.
Zdenek P. Bazant, Joong-Koo Kim
Materials and Structures, 1991, 24, 409-421.

[92.1] Creep and Shrinkage of High-Strength Concrete. A Test Report.
Henrik Elgaard Jensen
Department of Structural Engineering, Technical University of Denmark, 1992.

[92.2] Improved prediction model for time-dependent deformations of concrete: Part 3 - Creep at drying.
Zdenek P. Bazant, Joong-Koo Kim
Materials and Structures, 1992, 25, 21-28.

AFDELINGEN FOR BÆRENDE KONSTRUKTIONER
DANMARKS TEKNISKE HØJSKOLE

Department of Structural Engineering
Technical University of Denmark, DK–2800 Lyngby

SERIE R
(Tidligere: Rapporter)

Abonnement 1.7.1992 – 30.6.1993 kr. 130,–
Subscription rate 1.7.1992 – 30.6.1993 D.Kr. 130.–.

Hvis De ikke allerede modtager Afdelingens resumeoversigt ved udgivelsen, kan Afdelingen tilbyde at tilsende næste års resumeoversigt, når den udgives, dersom De udfylder og returnerer nedenstående kupon.

Returneres til
Afdelingen for Bærende Konstruktioner
Danmarks tekniske Højskole
Bygning 118
2800 Lyngby

Fremtidig tilsendelse af resumeoversigter udbedes af
(bedes udfyldt med blokbogstaver):

Stilling og navn: .....

Adresse: .....

Postnr. og -distrikt: .....

The Department has pleasure in offering to send you a next year's list of summaries, free of charge. If you do not already receive it upon publication, kindly complete and return the coupon below.

To be returned to:
Department of Structural Engineering
Technical University of Denmark
Building 118
DK-2800 Lyngby, Denmark.

The undersigned wishes to receive the Department's
List of Summaries:
(Please complete in block letters)

Title and name .....

Address.....

Postal No. and district.....

Country.....